Lecture #5

Metal-pipe Rectangular Waveguides (MPRWGs)

The main objective of this lecture is to explore modern methods of implementing this traditional guided-wave technology, for both low frequency and THz applications.

Low-loss Structures

Transmission Line Requirement

- Low loss/high Q for increased efficiency
  (since intrinsic material losses increase with frequency)
- High isolation
- Low in-band frequency dispersion
- Maximum achievable bandwidth
- Adequate power handling/thermal management
- Ease of integration (including antennas)
- Low-cost manufacturing

OVERVIEW

- Low-loss guided-wave structures
- Solutions to Maxwell's equations
  - TEmn mode waveguide
  - TEmno mode cavity resonator
- Substrate-integrated waveguides (SIWs)
  - Air-filled micromachined
  - Dielectric-filled micromachined
  - Photoimeagable thick-film
- Multi-chip modules (MCMs)
  - 60 GHz SIW/MMIC Receiver
  - THz MCMs
- REconfigurable THz INtegrated Architecture (RETINA)

Micromachined transmission lines for low loss

"Microshield line"

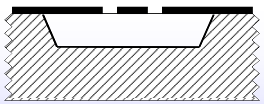

Suspended microstrip using back-face etching

Micromachined K-band Diplexer

- Highest Q for Non-Superconducting mm-Wave Planar Transmission Lines
- Q~460 @ 29 GHz

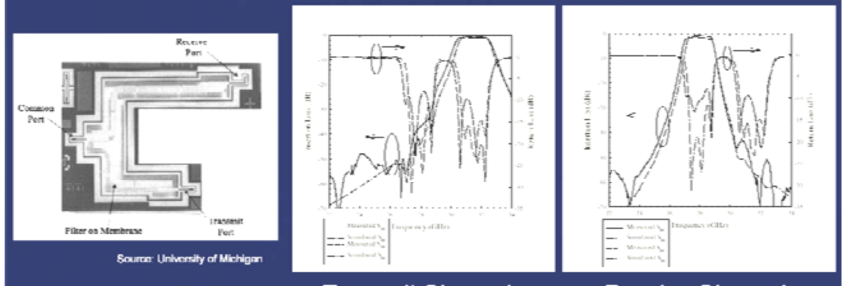

Transmit Channel *Receive Channel*

Radio Frequency Engineering
Lecture #5 MPRWGs

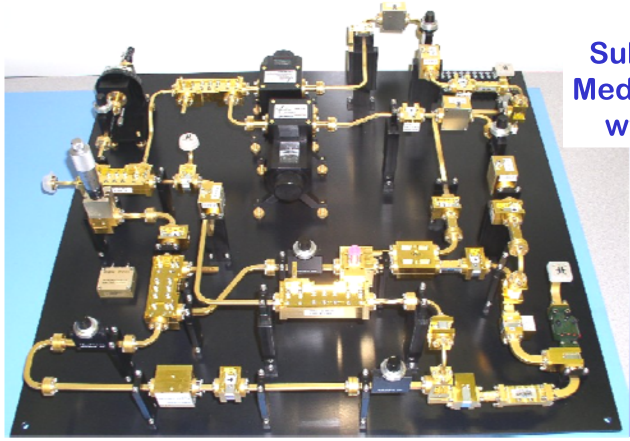

94 GHz Sub-system for Medical Research www.hxi.com

Imperial College London ステファン・ルシズィン Stepan Lucyszyn インペリアル・カレッジ・ロンドン准教授 UT-PSC

Radio Frequency Engineering
Lecture #5 MPRWGs

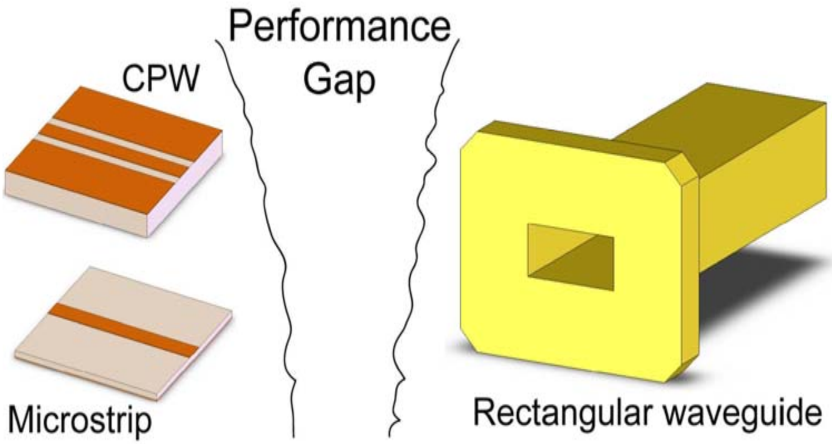

Imperial College London ステファン・ルシズィン Stepan Lucyszyn インペリアル・カレッジ・ロンドン准教授 UT-PSC

Radio Frequency Engineering
Lecture #5 MPRWGs

Air-filled Metal-Pipe Rectangular Waveguides

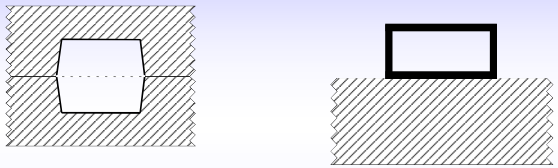

Bulk Micromachined (US):
JPL, Caltech
University of Arizona

Mar. 1993

Surface Micromachined (UK):
University of Bath

Sep. 1993

Imperial College London ステファン・ルシズィン Stepan Lucyszyn インペリアル・カレッジ・ロンドン准教授 UT-PSC

Maxwell's Equations

Modelling Guided-Wave Structures

When considering purely stead-state sinusoidal excitations, Maxwell's equations become:

$$\nabla x\hat{E} = -j\omega\mu\hat{H} \quad ...(1)$$
$$\nabla x\hat{H} = j\omega\varepsilon\hat{E} \quad ...(2)$$
$$\nabla \cdot \hat{E} = 0 \quad ...(3)$$
$$\nabla \cdot \hat{H} = 0 \quad ...(4)$$

In general,

$$\nabla x\hat{E} = -j\omega\mu\hat{H} \qquad \nabla x\hat{H} = j\omega\varepsilon\hat{E}$$

$$\frac{\partial E_z}{\partial y} - \frac{\partial E_y}{\partial z} = -j\omega\mu H_x \qquad \frac{\partial H_z}{\partial y} - \frac{\partial H_y}{\partial z} = j\omega\varepsilon E_x$$
$$\frac{\partial E_x}{\partial z} - \frac{\partial E_z}{\partial x} = -j\omega\mu H_y \qquad \frac{\partial H_x}{\partial z} - \frac{\partial H_z}{\partial x} = j\omega\varepsilon E_y$$
$$\frac{\partial E_y}{\partial x} - \frac{\partial E_x}{\partial y} = -j\omega\mu H_y \qquad \frac{\partial H_y}{\partial x} - \frac{\partial H_x}{\partial y} = j\omega\varepsilon E_y$$

Therefore, with a plane wave, one is left with the following:

$$\frac{\partial E_y}{\partial z} = j\omega\mu H_x \qquad \frac{\partial H_y}{\partial z} = -j\omega\varepsilon E_x$$
$$\frac{\partial E_x}{\partial z} = -j\omega\mu H_y \qquad \frac{\partial H_x}{\partial z} = j\omega\varepsilon E_y$$

It can be clearly seen that:

$$\frac{E_x}{H_y} = \frac{\gamma}{j\omega\varepsilon} = \frac{j\omega\mu}{\gamma} \equiv \eta \quad \text{i.e. intrinsic impedance of the medium}$$

also,

$$\frac{E_y}{H_x} = \frac{-\gamma}{j\omega\varepsilon} = \frac{j\omega\mu}{-\gamma} \equiv -\eta \quad \text{i.e. intrinsic impedance of the medium}$$

Note that the wave containing the fields (E_x and H_y) is independent of the wave containing (E_y and H_x).

Field Components in a Plane Wave

With a plane wave, there is only a variation in the field quantities in one dimension, e.g. the z direction of propagation:

$$\therefore \frac{\partial}{\partial x} = \frac{\partial}{\partial y} = 0$$

Mathematically, given the general expression $T_x\{f(x)\} = a\, f(x)$, where $T_x\{\ \}$ is an operator, $f(x)$ is a function of x and a is a constant then $f(x)$ is said to be an eigenfunction of $T_x\{\ \}$ with an eigenvalue equal to a. For example:

$f(z) = e^{-\gamma z}$ is an eigenfunction of the operator $\partial/\partial z$ with eigenvalue $-\gamma$, since

$$\partial/\partial z\left\{e^{-\gamma z}\right\} = -\gamma\, e^{-\gamma z}$$

$$\frac{\partial}{\partial z} \Rightarrow -\gamma = -jk_m \quad \left\{c.f.\frac{\partial}{\partial t} \Rightarrow +j\omega\right\}$$

Field Components in a Guided Wave

Within a guided wave, one is left with the following:

$$\nabla x\hat{E} = -j\omega\mu\hat{H} \qquad \nabla x\hat{H} = j\omega\varepsilon\hat{E}$$

$$\frac{\partial E_z}{\partial y} + \gamma E_y = -j\omega\mu H_x \qquad \frac{\partial H_z}{\partial y} + \gamma H_y = j\omega\varepsilon E_x$$
$$-\gamma E_x - \frac{\partial E_z}{\partial x} = -j\omega\mu H_y \qquad -\gamma H_x - \frac{\partial H_z}{\partial x} = j\omega\varepsilon E_y$$
$$\frac{\partial E_y}{\partial x} - \frac{\partial E_x}{\partial y} = -j\omega\mu H_z \qquad \frac{\partial H_y}{\partial x} - \frac{\partial H_x}{\partial y} = j\omega\varepsilon E_z$$

Re-arranging the first two equations in each column gives 2 pairs of simultaneous equations:

$$\frac{\partial E_z}{\partial y} = -\left(\gamma E_y + j\omega\mu H_x\right) \qquad \frac{\partial H_z}{\partial y} = -\left(\gamma H_y - j\omega\varepsilon E_x\right)$$
$$\frac{\partial E_z}{\partial x} = -\left(\gamma E_x - j\omega\mu H_y\right) \qquad \frac{\partial H_z}{\partial x} = -\left(\gamma H_x + j\omega\varepsilon E_y\right)$$

From these simultaneous equations it is possible to solve for all the fields in terms of E_z and H_z:

$$E_x = -\frac{1}{k_c^2}\left(\gamma\frac{\partial E_z}{\partial x} + j\omega\mu\frac{\partial H_z}{\partial y}\right)$$

$$E_y = +\frac{1}{k_c^2}\left(-\gamma\frac{\partial E_z}{\partial y} + j\omega\mu\frac{\partial H_z}{\partial x}\right)$$

$$H_x = -\frac{1}{k_c^2}\left(\gamma\frac{\partial H_z}{\partial x} - j\omega\varepsilon\frac{\partial E_z}{\partial y}\right)$$

$$H_y = -\frac{1}{k_c^2}\left(\gamma\frac{\partial H_z}{\partial y} + j\omega\varepsilon\frac{\partial E_z}{\partial x}\right)$$

Note that for plane waves $E_z = H_z = 0$.

Therefore, in a rectangular coordinate system:

$$\nabla^2\hat{E} = \frac{\partial^2\hat{E}}{\partial x^2} + \frac{\partial^2\hat{E}}{\partial y^2} + \frac{\partial^2\hat{E}}{\partial z^2} = -\omega^2\mu\varepsilon\hat{E}$$

In an orthogonal rectangular coordinate system:

$$\nabla^2 E_x = \frac{\partial^2 E_x}{\partial x^2} + \frac{\partial^2 E_x}{\partial y^2} + \frac{\partial^2 E_x}{\partial z^2} = -\omega^2\mu\varepsilon E_x$$

$$\nabla^2 E_y = \frac{\partial^2 E_y}{\partial x^2} + \frac{\partial^2 E_y}{\partial y^2} + \frac{\partial^2 E_y}{\partial z^2} = -\omega^2\mu\varepsilon E_y$$

$$\nabla^2 E_z = \frac{\partial^2 E_z}{\partial x^2} + \frac{\partial^2 E_z}{\partial y^2} + \frac{\partial^2 E_z}{\partial z^2} = -\omega^2\mu\varepsilon E_z$$

General Solution of the Wave Equation

In order to find a characteristic solution to Maxwell's equation, it is necessary to eliminate one of the two remaining field vectors. Thus, $\hat{H}$ can be eliminated as follows:

$$\nabla x(\nabla x\hat{E}) = \nabla x(-j\omega\mu\hat{H}) = -j\omega\mu(\nabla x\hat{H})$$

therefore:

$$\nabla x(\nabla x\hat{E}) = \omega^2\mu\varepsilon\hat{E}$$

but,

$$\nabla x(\nabla x\hat{E}) = \nabla(\nabla\cdot\hat{E}) - \nabla^2\hat{E}$$

now, rearranging, the E-field wave (propagation) equation can be obtained:

$\nabla^2\hat{E} + k_m^2\hat{E} = 0$ vector Helmholtz equation for an E-field in a homogeneous media

similarly, the H-field wave (propagation) equation can be obtained:

$\nabla^2\hat{H} + k_m^2\hat{H} = 0$ vector Helmholtz equation for a H-field in a homogeneous media

modified wavenumber, $k_m = \omega\sqrt{\mu\varepsilon}$

Plane Wave Solution

With a plane wave, there is a variation in the field quantities only in one dimension, e.g. the z direction of propagation:

$$\therefore \frac{\partial^2}{\partial x^2} = \frac{\partial^2}{\partial y^2} = 0 \quad \text{and} \quad \nabla^2\hat{E} = \frac{\partial^2\hat{E}}{\partial z^2} = -\omega^2\mu\varepsilon\hat{E} \quad \text{and}$$

$$\nabla^2 E_x = \frac{\partial^2 E_x}{\partial z^2} = -\omega^2\mu\varepsilon E_x$$

$$\nabla^2 E_y = \frac{\partial^2 E_y}{\partial z^2} = -\omega^2\mu\varepsilon E_y$$

$$\nabla^2 E_z = \frac{\partial^2 E_z}{\partial z^2} = -\omega^2\mu\varepsilon E_z$$

Now, considering only the E-field in the y direction, as it propagates along the z direction:

$$E_y = Ae^{-\gamma z} + Be^{+\gamma z} \quad where \quad \gamma = jk_m \quad and \quad k_m = \omega\sqrt{\mu\varepsilon}$$

A represents the amplitude of the forward travelling wave, while B represents the amplitude of the backward travelling wave.

This solution is identical to the voltage waves on a transmission line. In general, further analysis is usually confined to just the forward wave. When time dependency is also considered, the forward wave of the field is represented as: $E_x = E_o e^{(j\omega t - \gamma z)}$

Solution of Wave Equation for Guided-Wave Structures

The E-field component in the y direction, as it propagates along the z direction, is obtained from the wave equation :

$$\nabla^2 E_y = \frac{\partial^2 E_y}{\partial x^2} + \frac{\partial^2 E_y}{\partial y^2} + \frac{\partial^2 E_y}{\partial z^2} = -\omega^2 \mu\varepsilon E_y$$

The solution is obtained using the 'separation of variables' technique.
Now,

$$E_y = f(x,y,z) \quad \textit{and let} \quad E_y = f_1(x) f_2(y) f_3(z)$$

Therefore,

$$\nabla^2 E_y = f_1''(x) f_2(y) f_3(z) + f_1(x) f_2''(y) f_3(z) + f_1(x) f_2(y) f_3''(z) = -\omega^2 \mu\varepsilon\, f_1(x) f_2(y) f_3(z)$$

$$\therefore \frac{f_1''(x)}{f_1(x)} + \frac{f_2''(y)}{f_2(y)} + \frac{f_3''(z)}{f_3(z)} = -\omega^2\mu\varepsilon \equiv \gamma^2$$

TEmn Mode Waveguide

Boundary Conditions for MPRWG

For a perfectly conducting surface, the E-field parallel to the surface is zero. Given this, the analysis of a metal-pipe rectangular waveguide is essentially the superposition of two boundary conditions.

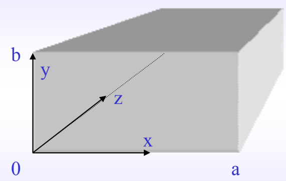

In the most general form:

$$f_1(x) = A\sin(k_x x) + B\cos(k_x x)$$

A solution for walls at x = [0, a] is:

$$k_x = m\frac{\pi}{a}$$

Similarly, if:

$$f_2(y) = C\sin(k_y y) + D\cos(k_y y)$$

A solution for walls at y = [0, b] is:

$$k_y = n\frac{\pi}{b}$$

A Fourier Transform in the z direction gives:

$$\gamma_x^2 + \gamma_y^2 + \gamma_z^2 = -k_m^2 \equiv \gamma^2 \quad \textit{where} \quad k_m \equiv \frac{\omega}{v_p} \quad \textit{and} \quad v_p = \frac{c}{\sqrt{\mu_r \varepsilon_r (1 - j\tan\delta)}}$$

where, γ_x, γ_y and $\gamma_{z \equiv} \gamma_g$ are constants, which may be complex numbers. Note that the left hand side represent the bound medium (i.e. the wave guide) and the right hand side represents the unbounded medium. Now, the cut-off modified wavenumber k_c, is given from the following:

$$\gamma_g^2 = \gamma^2 - \gamma_c^2 \quad \Rightarrow \quad k_g^2 = k^2 - k_c^2 \quad \textit{where}\ k_c = \sqrt{k_x^2 + k_y^2} \equiv \left.\frac{\omega_c}{v_p}\right|_{\text{LOSSLESS}}$$

$$\textit{Therefore} \quad \gamma_g = \pm\sqrt{(k_c^2 - k^2)}$$

Now,

$$\frac{f_3''(z)}{f_3(z)} \equiv \gamma_g^2 \quad \textit{and if} \quad f_3(z) = E_y(z) = e^{-\gamma_g z} \quad \textit{then} \quad \frac{\partial^2 E_y(z)}{\partial z^2} = \gamma_g^2 E_y(z)$$

The solution of the wave equation takes the form:

$$E_y = f_1(x) f_2(y) e^{(j\omega t - \gamma_g z)}$$

An E-field that is tangential to a lossless conducting wall must vanish at this boundary. Therefore, the solution of the wave equation for the E-field component in the y direction, as it propagates along the z direction, is obtained with B = C = 0:

$$E_y = E_o \sin\left(m\frac{\pi}{a}x\right)\cos\left(n\frac{\pi}{b}y\right)e^{(j\omega t - \gamma_{mn} z)}$$

An H-field that is normal to the conducting wall must vanish at this boundary. Therefore, the solution of the wave equation for the H-field component in the x direction, as it propagates along the z direction, is obtained with B = C = 0:

$$H_x = H_o \sin\left(m\frac{\pi}{a}x\right)\cos\left(n\frac{\pi}{b}y\right)e^{(j\omega t - \gamma_{mn} z)}$$

The solution of the wave equation for H-field component in the z direction, as it propagates along the z direction, is obtained with A = C = 0:

$$H_z = -jH_o \cos\left(m\frac{\pi}{a}x\right)\cos\left(n\frac{\pi}{b}y\right)e^{(j\omega t - \gamma_{mn} z)}$$

For Ey, Hx and Hz, each combination of (m, n) constitutes a separate solution to Maxwell's equations for the given boundary conditions. Mathematically, each independent solution is an eigenfunction of this problem and the values for kx and ky are the eigenvalues. In physical terms, each solution gives rise to a different mode of propagation within the metal-pipe rectangular waveguide.

Field and current patterns in the TE_{10} (H_{10}) and TM_{11} (E_{11}) modes in a square cross-sectional waveguide. The H-field lines are in GREEN, the E-field lines are in RED, and the currents in the guide walls are in BLUE.

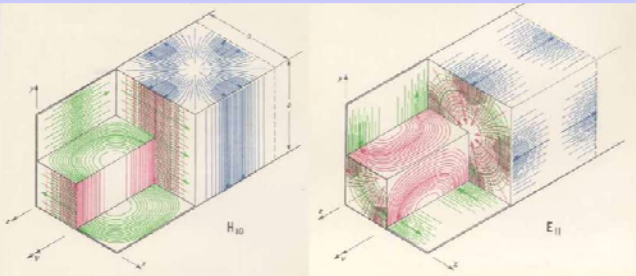

Originally, the British called a TE mode an "H mode". In a TE mode there is no longitudinal E-field, but there is a longitudinal H-field. However you can see that in the TE mode there is also a transverse component of H-field. The British thought that the unique longitudinal H-field was a better descriptor than the transverse electric field with no longitudinal E-filed component.

Radio Frequency Engineering
Lecture #5 MPRWGs

Resonant Cavity Box Modes

$$\gamma_x^2 + \gamma_y^2 + \gamma_z^2 = -\left(\frac{\omega}{v_p}\right)^2$$

$$\therefore \omega = v_p \sqrt{\left(k_x^2 + k_y^2 + k_z^2\right)}$$

but if :

$$k_z = l\frac{\pi}{c}$$

$$\therefore f_o = v_p \sqrt{\left(\frac{m}{2a}\right)^2 + \left(\frac{n}{2b}\right)^2 + \left(\frac{l}{2c}\right)^2}$$

Imperial College London ステファン・ルシズィン Stepan Lucyszyn
インペリアル・カレッジ・ロンドン准教授 UT-PSC

Radio Frequency Engineering
Lecture #5 MPRWGs

TEmno Mode Cavity

Now, the cut-off wavelength is given by:

$$k_c = \sqrt{k_x^2 + k_y^2} = \sqrt{\left(m\frac{\pi}{a}\right)^2 + \left(n\frac{\pi}{b}\right)^2} \equiv \frac{2\pi}{\lambda_c}$$

$$\therefore \lambda_c = \frac{1}{\sqrt{\left(\frac{m}{2a}\right)^2 + \left(\frac{n}{2b}\right)^2}}$$

For example, with the TE_{10} mode, m = 1 and n = 0:

$$\lambda_c = 2a \quad \therefore f_c = \frac{v_p}{\lambda_c} \Rightarrow \frac{c}{2a} \quad \text{for an air-filled waveguide}$$

Also, it can be easily proven that:

$$\lambda_g = \frac{\lambda}{\sqrt{1-\left(\frac{f_c}{f}\right)^2}}$$

Imperial College London ステファン・ルシズィン Stepan Lucyszyn
インペリアル・カレッジ・ロンドン准教授 UT-PSC

Radio Frequency Engineering
Lecture #5 MPRWGs

TE101 box mode E- and H-fields within a MPRWG

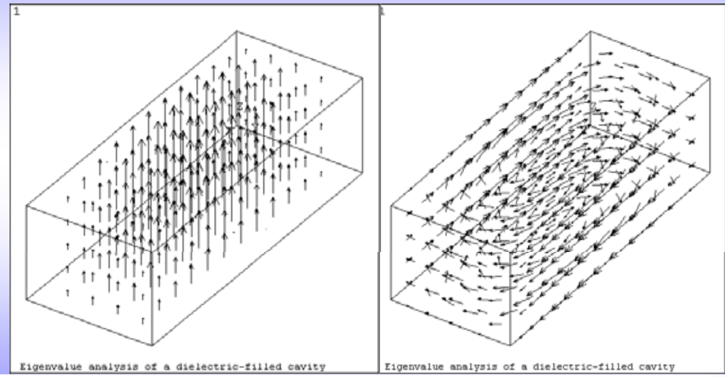

Imperial College London ステファン・ルシズィン Stepan Lucyszyn
インペリアル・カレッジ・ロンドン准教授 UT-PSC

Air-filled Micromachined

Micromachined Cavity Resonator

- Fabrication
  - Bulk Micromachining
  - Wafer Bonding
- High Q
  - MCO ~130
  - FRO ~ 20
- Low Phase Noise
  - -85 dB @100 KHz
  - -110 dB @ 110 MHz
- Frequency = 33 GHz

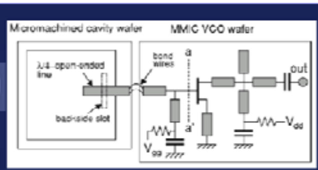

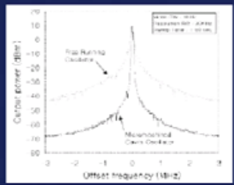

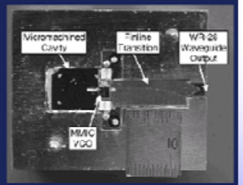

University of Seoul

Radio Frequency Engineering
Lecture #5 MPRWGs

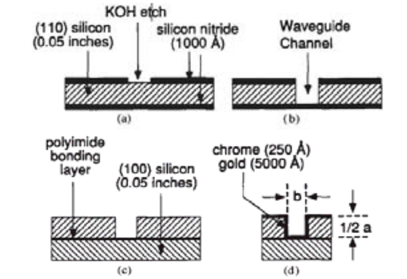

Cross-section view of the fabrication process. (a) Si_3N_4 mask defines the waveguide height. (b) Wafer is etched completely through. (c) Wafer with waveguide channels is bonded to an unetched wafer which forms the waveguide side wall. (d) Completed half-section of waveguide with gold plating. Two of these sections are mated to form the waveguide. "a" is the waveguide width and "b" is the height.

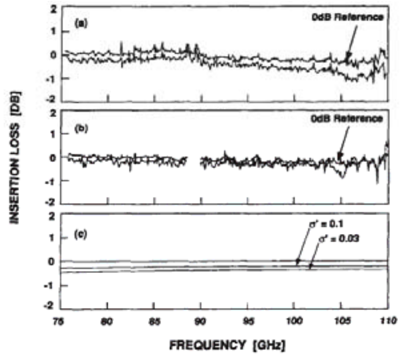

(a) Measured loss of a 2.5-cm long section of Si-based WR-10 waveguide. The surface of the silicon was metallized with approximately 3 μm of gold to reduce RF losses. (b) Measured loss of a 2.5-cm long section of conventional metallic waveguide (the small gap in the data near 90 GHz is due to an instability in the BWO). (c) Calculated loss of a 2.5-cm long section of waveguide for two different values of conductivity σ' normalized to copper.

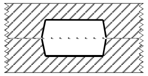

Imperial College London ステファン・ルシズィン Stepan Lucyszyn
インペリアル・カレッジ・ロンドン准教授
UT-PSC

Radio Frequency Engineering
Lecture #5 MPRWGs

The metal-pipe rectangular waveguide can be considered as the ultimate guided-wave structure, although package density is poor. The University of California first proposed the idea of implementing air-filled metal-pipe rectangular waveguides, using integrated circuit technology, back in 1980:

Rutledge, D. B. , Schwarz, S.E., Hwang, T. L. , Angelakos, D. J. , Mei, K.K., and Yokota, S.: **'Antennas and waveguides for far-infrared integrated circuits',** IEEE J. Quantum Elec.., **1980**, 16, pp.508–516

More than a decade later, in collaboration with the University of Arizona, the California Institute of Technology demonstrated a W-band micromachined air-filled metal-pipe rectangular waveguide. By using a two-wafer sandwich approach (measured level of insertion loss of only 0.04 dB/λg at 100 GHz):

W. R. McGrath, C. Walker, M. Yap, and Y.-C. Tai, **"Silicon micromachined waveguides for millimeter-wave and submillimeter- wave frequencies",** IEEE Microwave & Guided Wave Letters, vol. 3, no. 3, **Mar. 1993**

0.1 THz

Wafer-bonding continues to advance, with vertically integrated micromachined filters being demonstrated at frequencies as low as 10 GHz:

Harle, L., and Katehi, L.P.B.: **'A vertically integrated micromachined filter',** IEEE Trans. Microwave Theory Tech., 2002, 50, (9), pp.20 63–2068

Imperial College London ステファン・ルシズィン Stepan Lucyszyn
インペリアル・カレッジ・ロンドン准教授
UT-PSC

Radio Frequency Engineering
Lecture #5 MPRWGs

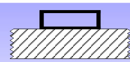

Surface micromachining technology has evolved from multilayer microfabrication; the difference being that sacrificial layers are used. Micromachining is generally not applied to the substrate material, but on the dielectric and/or conductive layers above it. For example, the University of Bath reported a 600 GHz air-filled metal-pipe rectangular waveguide structure, realised using just a single wafer:

Treen, S.A., and Cronin, N.J.: **'Terahertz metal pipe waveguides'.** Proc.18th International Conference on Infrared and Millimetre Waves, London, **Sep. 1993**, pp.470–471

A very thick layer of SU-8 photoresist was used to define the waveguide. After gold was deposited onto an SU-8 former, the sacrificial layer of SU-8 was removed to leave a 3D metal structure.

This let to the work of the Terahertz Integrated Technology Initiative Network (TINTIN) project:

J. W. Digby, C. E. McIntosh, G. M. Parkhurst, B. M. Towlson, S. Hadjiloucas, J. W. Bowen, J. M. Chamberlain, R. D. Pollard, R. E. Miles, D. P. Steenson, L. S. Karatzas, N. J. Cronin and S. R. Davies, **"Fabrication and characterization of micromachined rectangular waveguide components for use at millimeter-wave and terahertz frequencies",** IEEE Transactions on Microwave Theory and Techniques, "vol.48, no. 8., Aug. 2000

Imperial College London ステファン・ルシズィン Stepan Lucyszyn
インペリアル・カレッジ・ロンドン准教授
UT-PSC

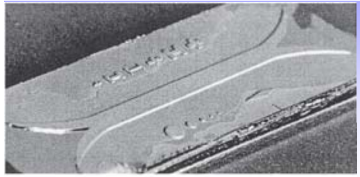

0.2 THz

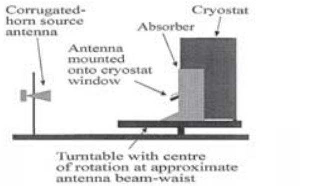

Photograph of micromachined waveguide with antennas.

Experimental setup for far-field measurements on the integrated horn

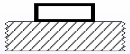

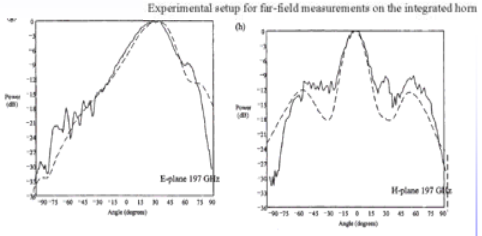

Measured (continuous line) and simulated (dashed line) E-plane and corresponding H-plane co-polar far-field patterns for the integrated antenna at 150, 165, 180, and 197 GHz.

TINTIN Project (UK):
University of Bath
University of Leeds
University of Nottingham
University of Reading

Radio Frequency Engineering
Lecture #5 MPRWGs

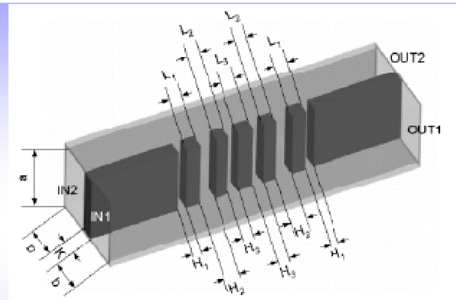

Waveguide hybrid coupler at 1.3 THz

A. Pavolotsky, et al.
Microelectronics J, Vol. 36, 2005

Imperial College London ステファン・ルシズィン Stepan Lucyszyn インペリアル・カレッジ・ロンドン准教授 UT-PSC

Radio Frequency Engineering
Lecture #5 MPRWGs

THz Rectangular Waveguide Receiver

H. Kazemi, *et al.* Int. J. Infrared and Millimetre Waves, 1999

TINTIN Project

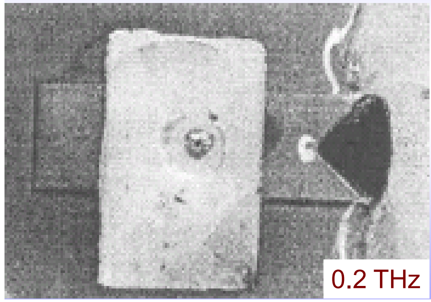

0.2 THz

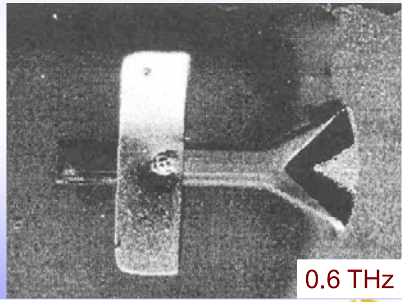

0.6 THz

Imperial College London ステファン・ルシズィン Stepan Lucyszyn インペリアル・カレッジ・ロンドン准教授 UT-PSC

Radio Frequency Engineering
Lecture #5 MPRWGs

Micromachined Waveguide Antennas at 1.6 THz

J.W. Bowen, *et al.*
IET Electronics Letters,
vol. 42, no. 15, 2006

TINTIN Project

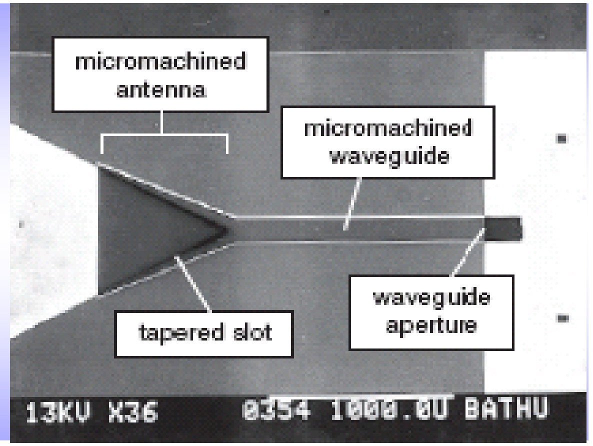

Imperial College London ステファン・ルシズィン Stepan Lucyszyn インペリアル・カレッジ・ロンドン准教授 UT-PSC

THz Rectangular Waveguide Array at 3 THz

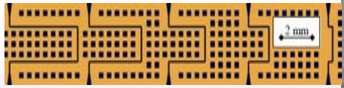

C.D. Nordquist, *et al.* AP-S 2008

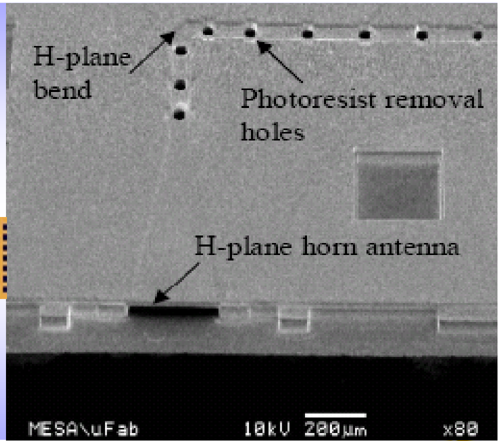

S. Lucyszyn, D. Budimir, Q. H. Wang and I. D. Robertson, **"Design of compact monolithic dielectric-filled metal-pipe rectangular waveguides for millimetre-wave applications"**, *IEE Proceedings – Microwaves, Antennas and Propagation*, vol. 143, no. 5, pp. 451-453, Oct. 1996

S. Lucyszyn, **"The future of on-chip terahertz metal-pipe rectangular waveguides implemented using micromachining and multilayer technologies"**, *IEE Colloquium Digest on Terahertz Technology and its Applications*, London, pp. 10/1-10, Apr. 1997

S. Lucyszyn, D. Budimir and I. D. Robertson, **"Design of low-loss monolithic millimetre-wave filters using dielectric-filled metal-pipe rectangular waveguides"**, *Proceedings of the ESA Workshop on Advanced CAD for Microwave Filters and Passive Devices*, ESTEC, Noordwijk, The Netherlands, pp. 381-387, Nov. 1995

S. Lucyszyn, Q. H. Wang and I. D. Robertson, **"0.1 THz rectangular waveguide on GaAs semi-insulating substrate"**, *IEE Electronics Letters*, vol. 31, no. 9, pp. 721-722, Apr. 1995

S. Lucyszyn, **"Multilayer and micromachined passive components"**, *IEE Tutorial Colloquium Digest on Design of RFICs and MMICs*, London, pp. 8/1-7, Nov. 1999

Dielectric-filled Micromachined

Miniature MPRWG Technologies

* Monolithic micromachining techniques have been investigated for realising air-filled MPRWG structures up to 3 THz

* Potential drawbacks with this micromachining technology are the limitations in design flexibility, poor yield and high production cost.

* Experimental multilayer MPRWGs have been demonstrated.

* In principle the multilayer MPRWG technology allows complete integration of waveguides, lumped elements and microstrip with a fixed process sequence.

First Reported Dielectric-filled Metal-pipe Rectangular Waveguide (Lucyszyn, *et al.,* IEE ,1995)

Experimental Platform Restrictions:

* **Only three 1 μm thick metal and two 2 μm thick dielectric layers**
* **Only aluminium metal and polyimide dielectric materials**
* **Only on-wafer probed measurements and, therefore, π-network**
* **Cut-off frequency confirmation of TE10 mode propagation required**

$$Z_o = 2\frac{b}{a}Z_{TE}$$

$$Z_{TE} = j\frac{\omega\mu}{\gamma}$$

$$\gamma^2 = \Gamma_d^2 - j\frac{2Z_s}{\omega\mu b}\left[\left(\frac{\Gamma_d}{k_c}\frac{m\pi}{a}\right)^2 - k_c^2\left(1+\frac{2b}{a}\right)\right]$$

where

$$\Gamma_d^2 = k_c^2 - k_{od}^2$$
$$k_c = \omega_c\sqrt{\mu\varepsilon}$$
$$k_{od} = \omega\sqrt{\mu\varepsilon(1-j\tan\delta)}$$
$$Z_s = \text{surface impedance}$$

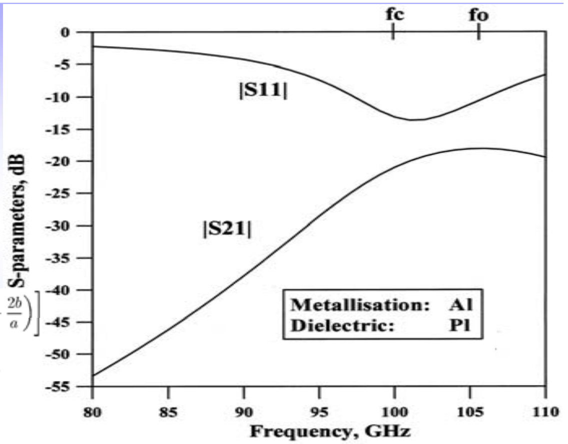

Radio Frequency Engineering
Lecture #5 MPRWGs

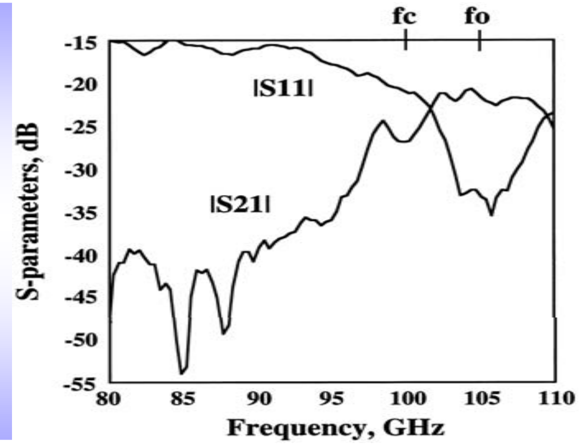

Imperial College London
ステファン・ルシズィン Stepan Lucyszyn
インペリアル・カレッジ・ロンドン准教授
UT-PSC

Radio Frequency Engineering
Lecture #5 MPRWGs

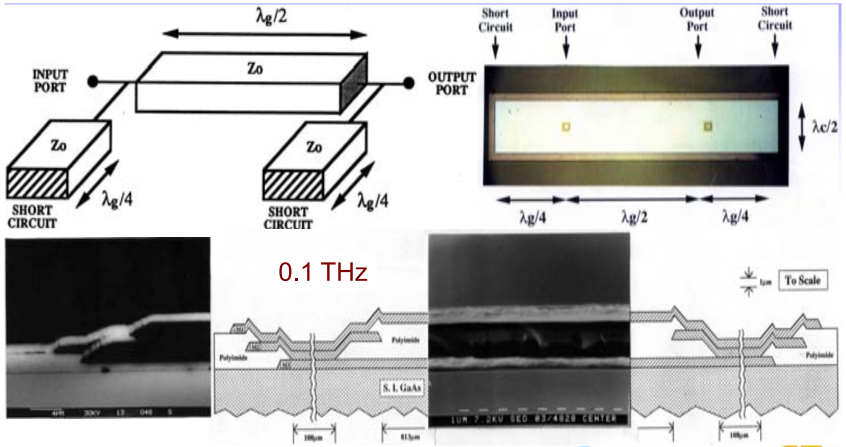

Imperial College London
ステファン・ルシズィン Stepan Lucyszyn
インペリアル・カレッジ・ロンドン准教授
UT-PSC

Radio Frequency Engineering
Lecture #5 MPRWGs

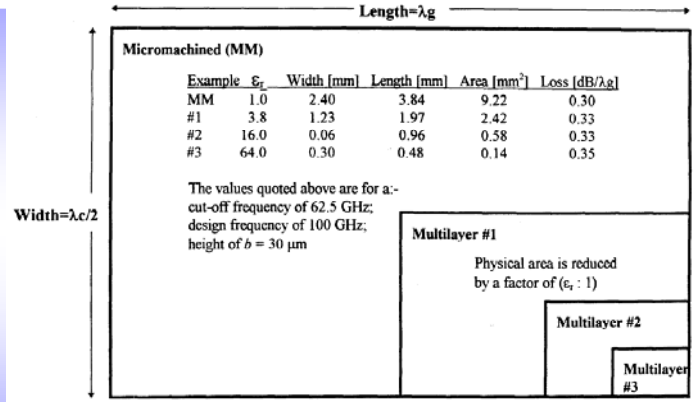

Example	ε_r	Width [mm]	Length [mm]	Area [mm^2]	Loss [dB/λg]
MM	1.0	2.40	3.84	9.22	0.30
#1	3.8	1.23	1.97	2.42	0.33
#2	16.0	0.06	0.96	0.58	0.33
#3	64.0	0.30	0.48	0.14	0.35

The values quoted above are for a:-
cut-off frequency of 62.5 GHz;
design frequency of 100 GHz;
height of b = 30 μm

Physical area required for a λg section of MPRWG (to scale)

Imperial College London
ステファン・ルシズィン Stepan Lucyszyn
インペリアル・カレッジ・ロンドン准教授
UT-PSC

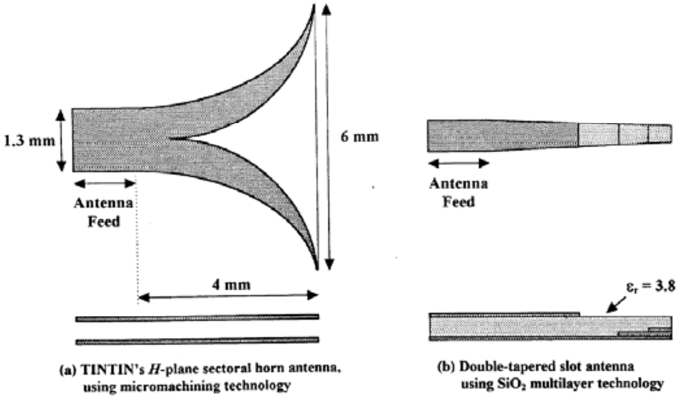

MPRWG antenna designs for 200 GHz operation (to scale)

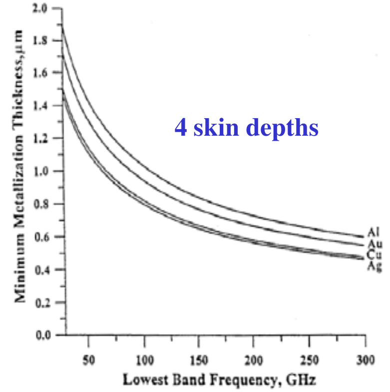

Recommended minimum metallisation thickness

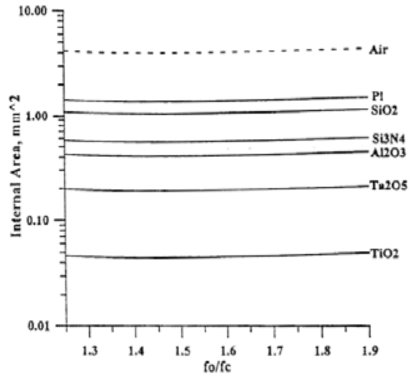

Internal area of a λg length of line at 150 GHz

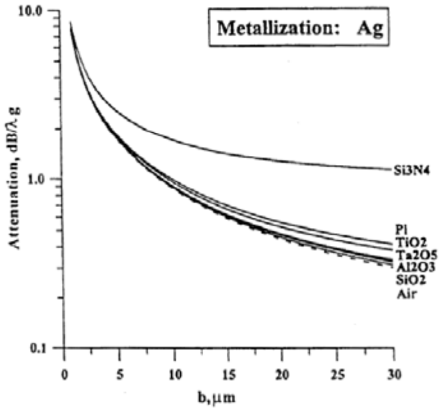

Dielectric dependent attenuation curves

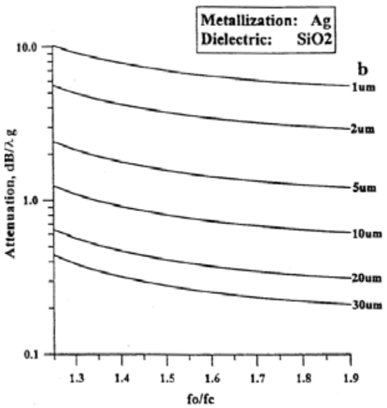

Cross-section dependent attenuation curves

Design for 150 GHz:
- Thick metal and thick dielectric layers
- Silver and fused quartz materials
- Only on-wafer probed measurements and, therefore, π-network
- Operating well-away from cut-off, with fo/fc = √2=1.414

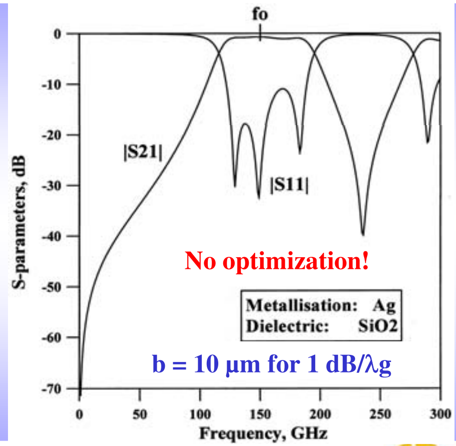

Substrate Integrated Folded Waveguides (SIFWs)

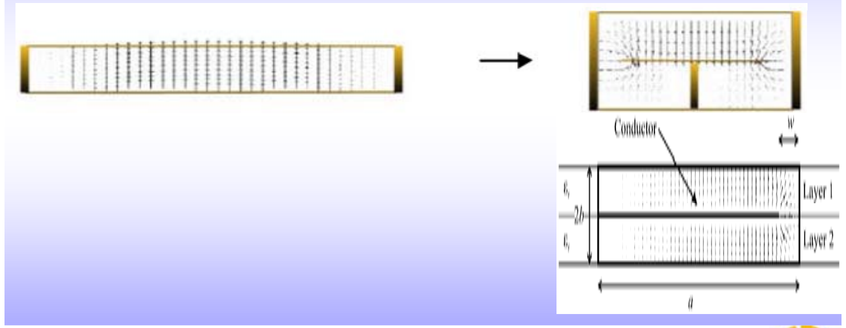

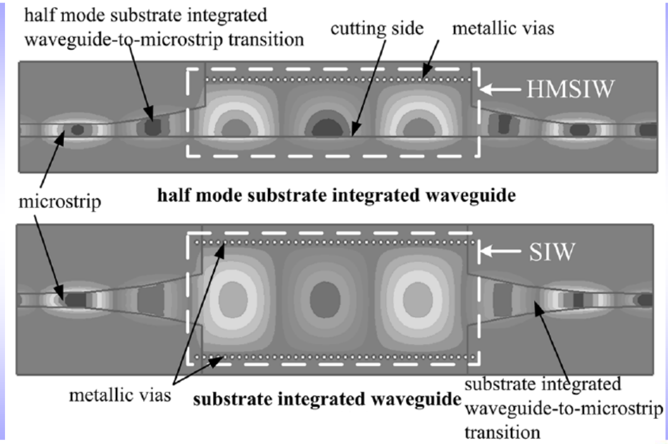

Post-wall Waveguide

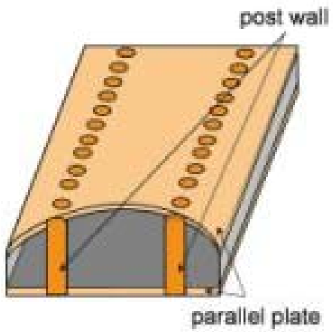

Slot Antenna

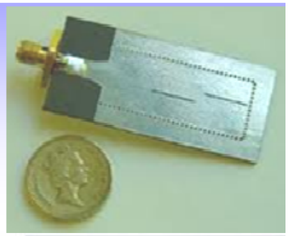

filter

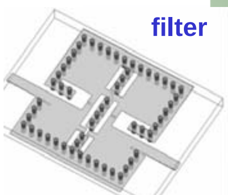

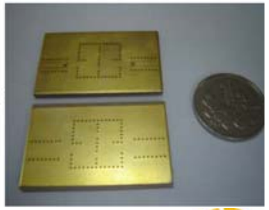

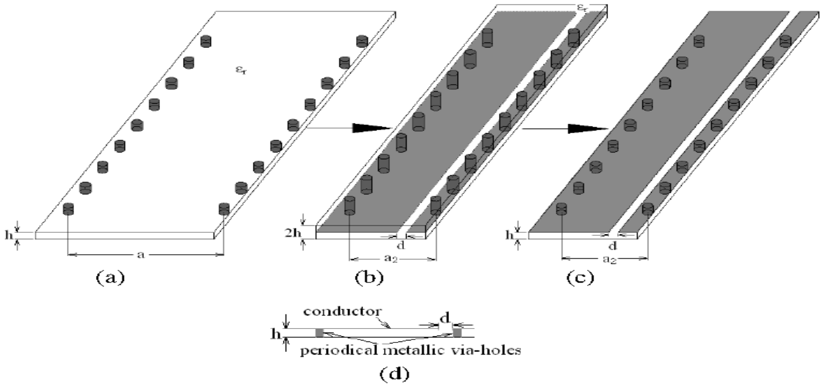

Figure 1. Configuration of SIW, SIFW and HMSIFW: (a) SIW, (b) SIFW, (c) HMSIFW, (d) the side view of the HMSIFW.

Photoimageable Thick-film

Aftanasar, M.S.; Young, P.R.; Robertson, I.D. (2002) **Rectangular Waveguides in Thick Film Photoimageable Technology**: IEE Colloquium on Thick Film Technology for Microwave Applications

M. S. Aftanasar, P. R. Young, I. D. Robertson and **S. Lucyszyn**, **"Fabrication of dielectric-filled rectangular waveguide using thick-film processing"**, *6th IEEE High Frequency Postgraduate Colloquium Digest*, Cardiff, pp. 82-87, Sep. 2001

M. S. Aftanasar, P. R. Young, I. D. Robertson, J. Minalgiene and **S. Lucyszyn**, **"Photoimageable thick-film millimetre-wave metal-pipe rectangular waveguides"**, *IEE Electronics Letters*, vol. 37, no. 18, pp. 1122-1123, Aug. 2001

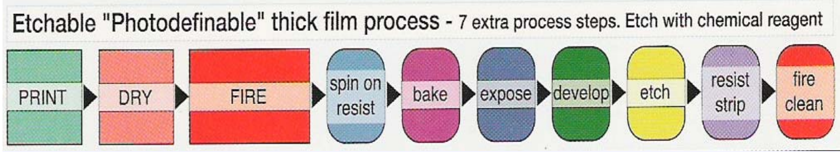

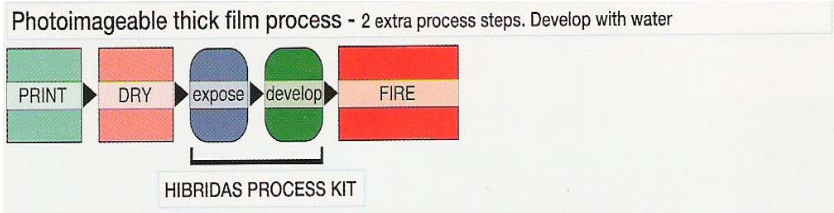

What about Screen Printing?

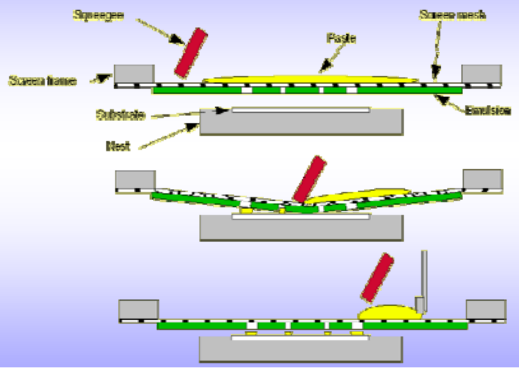

SC8 Spin Developer and MA4 Exposure Unit

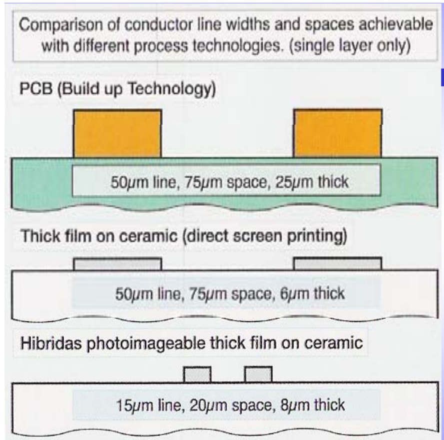

Hibridas Photoimageable Thick Film on Ceramic

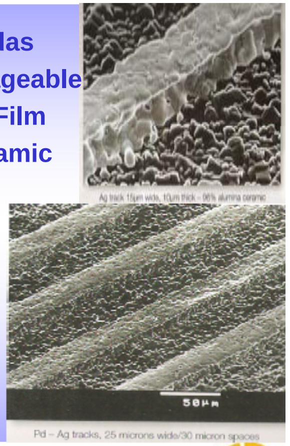

Attenuation of the Dielectric-Filled Rectangular Waveguide [dB/mm]

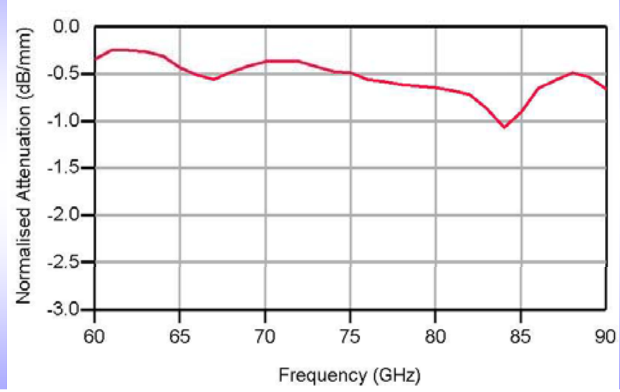

Photoimageable Thick-film Waveguides

2.490 mm Through Line **4.010 mm 270° Delay Line**

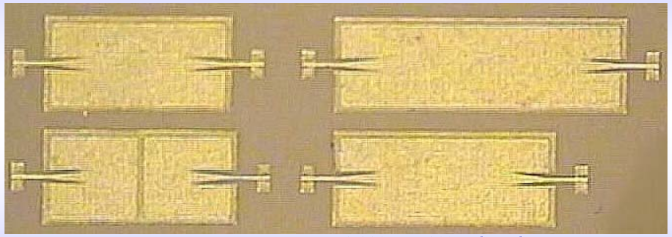

CPW Probe Pads

Two 1.245 mm Off-Set Shorts **2.990 mm 90° Delay Line**

- **18 µm thick photosensitive dielectric**
- **6 µm thick photosensitive gold conductor**

*** 0.5 dB/mm loss across the 60 to 80 GHz range**

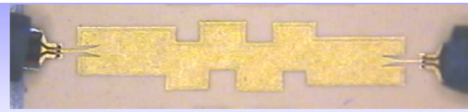

165 GHz Filter

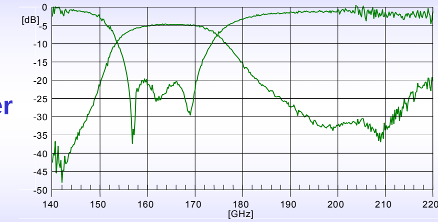

Stephens, D.; Young, P.R.; Robertson, I.D. (2005) **Millimeter-wave substrate integrated waveguides and filters in photoimageable thick-film technology.** IEEE Transactions on Microwave Theory and Techniques, 53(12), pp.3832-3838.
Aftanasar, M.S.; Young, P.R.; Robertson, I.D. (2002) **Rectangular waveguide filters using photoimageable thick-film processing,** 32nd European Microwave Conference, Milan, Italy

TRL Calibration

Thru

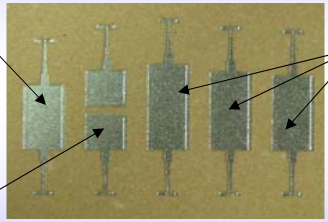

Reflect

Line standards at $\lambda_g/4$ at start, end, and mid-frequencies of waveguide

TFMS – Waveguide Transition

180 GHz Filter – Measured Results

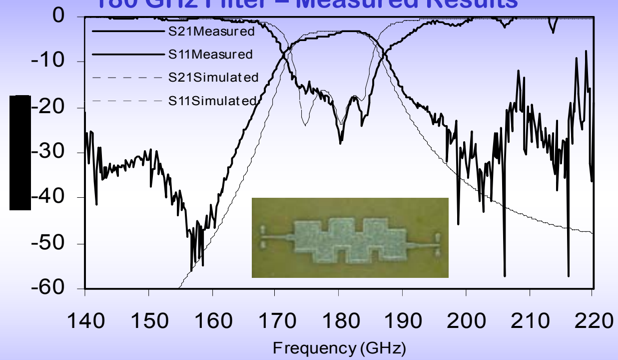

Stephens, D.; Young, P.R.; Robertson, I.D., **"Design and characterization of 180 GHz filters in photoimageable thick-film technology"** IEEE MTT-S IMS, 2005, vol. 1, pp. 451-454

V-band Waveguide Back-to-back Transition Measurements

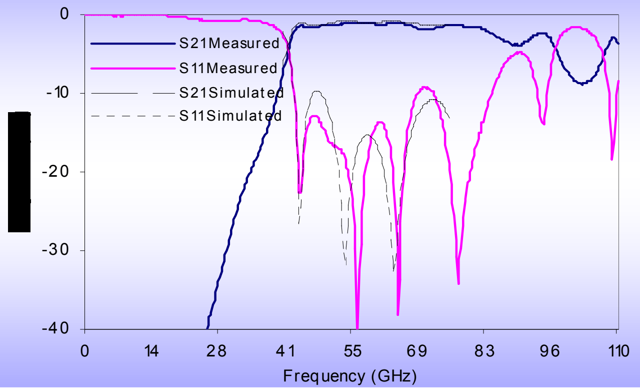

W-band (75-110 GHz) Antenna

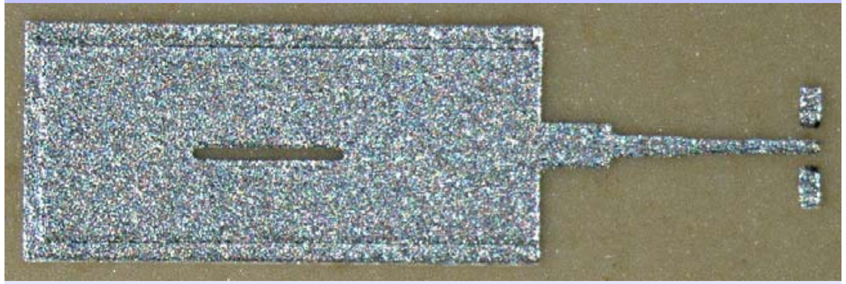

Stephens, D.; Young, P.R.; Robertson, I.D. (2005) **W-band substrate integrated waveguide slot antenna.** Electronics Letters, 41(4), pp.165-167.

MCMs

Multi-chip Modules

Hybrid Circuit

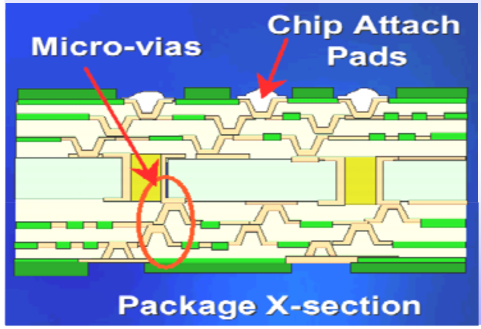

Monolithic Circuit

Interconnect stack in the Intel 130nm P860 technology

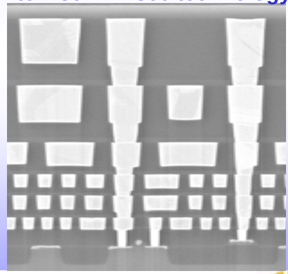

MCM Technologies

✍ The system-on-chip concept falls down in many cases when superior performance can only be obtained with different device technologies

✍ The MCM approach is to partition the system with the best component for the task: CMOS for digital functions, pHEMT MMICs for mm-wave functions, etc.

✍ The MCM combine the chips into a single module containing all the interconnects, bias circuitry, filters and other passive components (even a planar antenna)

✍ This compromise approach should be chosen wherever possible for low-cost, high volume, manufacturing

Difficulties in Implementing System-on-Chips (SoCs):

*** Integration of low phase noise oscillators**
(i.e. achieving high Q-factor resonators)
*** Integrating high-selectivity passive filters**
(i.e. achieving high Q-factor components)
*** Achieving high transmitter efficiency**
(i.e. optimal impedance matching and power combining)
*** Integration of high efficiency antennas**
*** Integrating the diplexing function**
*** Minimising coupling and leakage**
*** Implementing RF and baseband on a single chip**
*** Ensuring adequate decoupling for DC bias lines**

✍ MCMs can be simply implemented at microwave frequencies in the same way as a hybrid MIC is created

✍ At these frequencies, bond-wires usually connect chips to their carrier. Microstrip is preferred on both the carrier and MMIC, because they have simple propagation modes

✍ At mm-wave frequencies flip-chip (i.e. solder bump) mounting is employed, where the MMIC is placed upside down. CPW is preferred on both the carrier and MMIC

✍ There are 3 more advanced MCM technologies:

- MCM-D (Deposited), thin-film deposition for small feature sizes, as used by Intarsia
- MCM-L (Laminated) organic substrates for high volume large board and ultra-low cost
- MCM-C (Ceramic), with co-fired ceramics (e.g. LTCC) for high RF performance
- Thick-Film (screen printed), with new photoimageable materials available
- MCM-H (Hybrid), a mixture of above

✍ MCM-D uses normal spinning, thin-film metal deposition and photolithographic procedures to fabricate multilayer passive components and interconnects with 10 μm feature sizes

∗ This offers highest performance and is best suited to flip-chip assembly, EXPENSIVE !!!!!

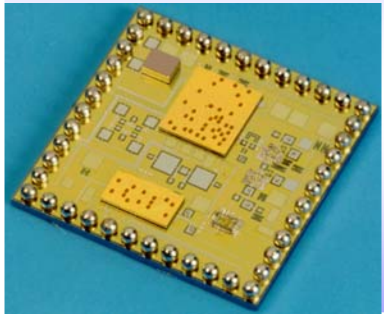

5.25 GHz Hiperlan transceiver MCM (employing flip-chip silicon and GaAs MMICs)

Courtesy of David J. Pedder, formerly Intarsia Corp.

✍ MCM-C technology employs ceramic materials in their un-fired ("green") state in the form of tapes or pastes

- multi-layer modules are formed from multiple layers of tapes, or multiple thick-film screen-prints of the pastes, and then the layers are all fired together. This includes low-temperature co-fired ceramic (LTCC) technology.
- micro-vias formed by punching or laser drilling
- new materials are photoimageable

✍ MCM-L technology is essentially a very advanced laminated PCB technology

- multiple layers are formed by laminating successive layers, with photolithographic procedures being applied at each stage to define the metal patterns (copper etching process)
- micro-vias are formed by mechanical punching or laser machining
- MCM-L technology is capable of making microstrip lines with approximately 40 μm minimum feature sizes
- large boards can be processed
- can be used in mm-wave modules (PTFE)

Conceptual LTTC module (Murata)

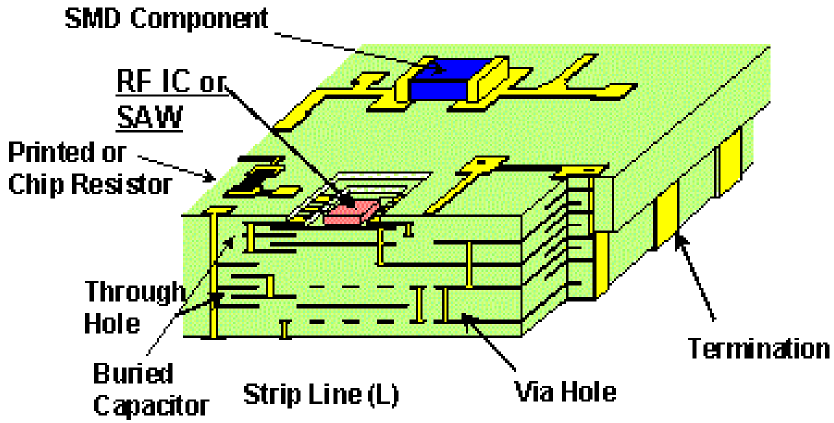

LTCC Process

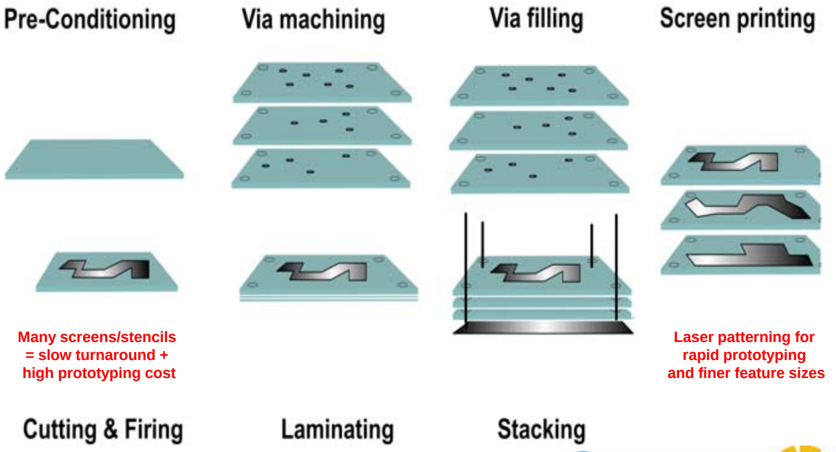

HeraLock™ by Heraeus (self-constraining tape)

Awarded the Number One Ceramic Accomplishment for 2002 at International Microelectronic and Packaging Society (IMAPS) (18cm x 28 cm panel)

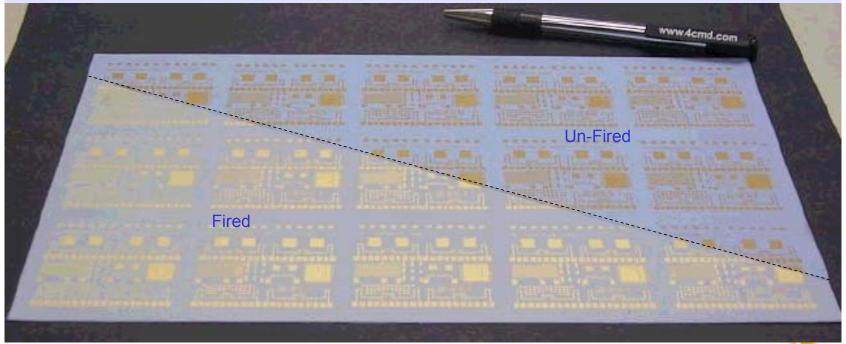

Special Advantages LTCC Technology:

* Embedded passives
* 3D structures
* High density of interconnects
* Strength and rigidity
* Good thermal performance
* Parallel processing
* Competitive cost (now comparable to FR4)

Structures Possible with HeraLock™

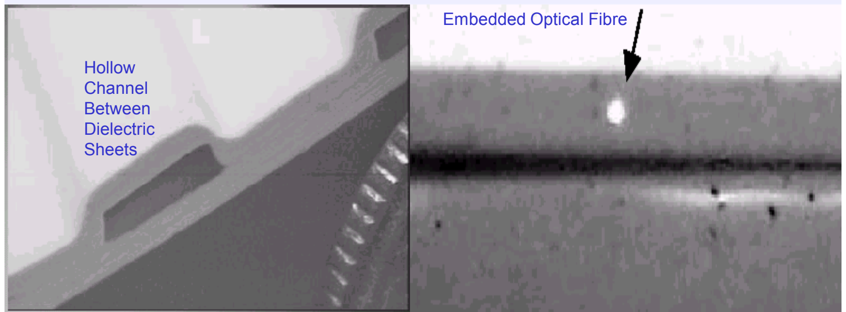

60 GHz SIW/MMIC Receiver

Robertson, I.D.; Samanta, K.K., **"Multilayer thick-film photoimageable technology for 60 GHz system-in-package"**, APMC 2008. Asia-Pacific Microwave Conference, 16-20 Dec. 2008, pp.1-4

Samata, K.; Stephens D.; Robertson, I.D. (2007) **Design and Performance of a 60 GHz Multi-Chip Module Receiver Employing Substrate Integrated Waveguides.** IET Microwaves, Antennas & Propagation, 1(5), pp.961-967

Samanta, K.K.; Stephens, D.; Robertson, I.D. (2006) **60 GHz multi-chip-module receiver with substrate integrated waveguide antenna and filter.** Electronics Letters, 42(12), pp.701-702.

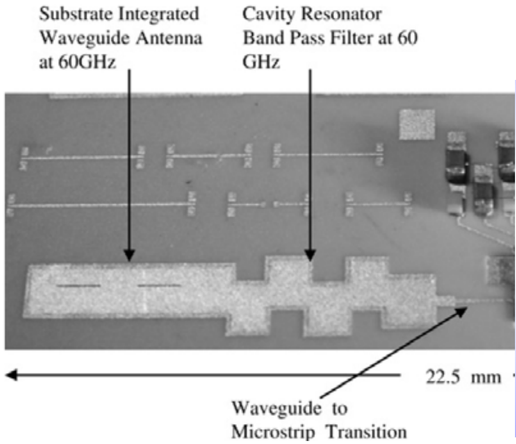

60 GHz Filter

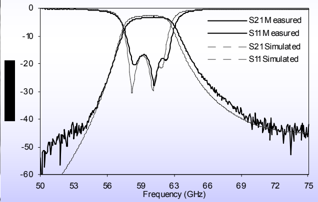

60 GHz Receiver Using Photoimageable Thick Film Materials

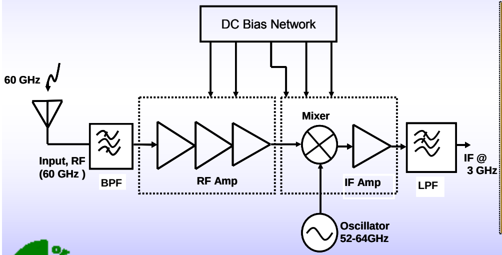

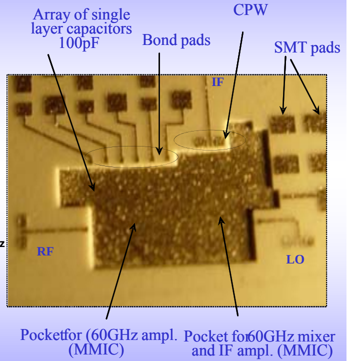

60 GHz SIW Slot Antenna

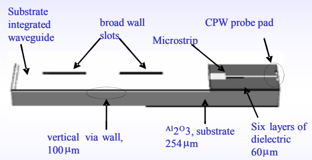

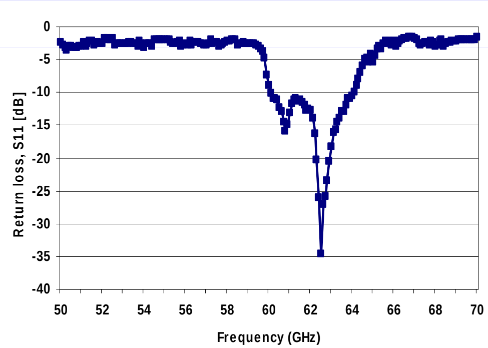

Complete SIW/MMIC 60GHz Receiver

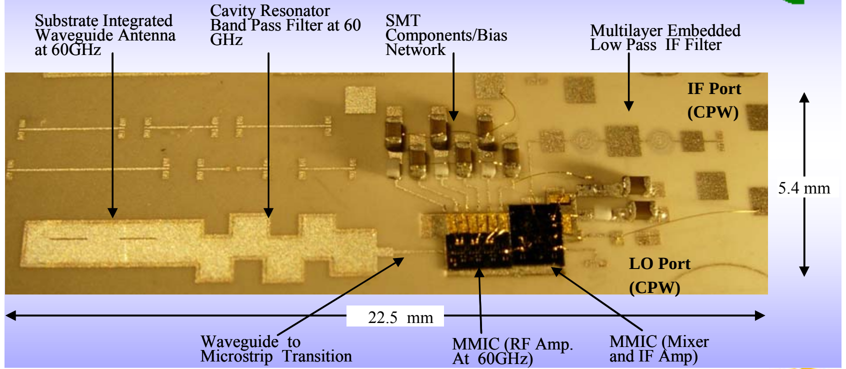

Pros:
- Thick-film processing is simple
- Offers multi-layer processing
- SIW can be lowest loss
- Propagation characteristics accurately predictable at mm-wavelengths
- Printing instead of laminating (e.g. LTCC) gives less restrictions on layout & cavities are easily made

Cons:
- tan δ of dielectric contributes to losses
- Reduced height of the waveguide contributes to losses
- Circuit is susceptible to layer misalignment during processing affecting performance
- Serial processing; many print / expose / develop steps
- Conductor definition not as good as thin film

Receiver Radiation Pattern Measured & Modelled

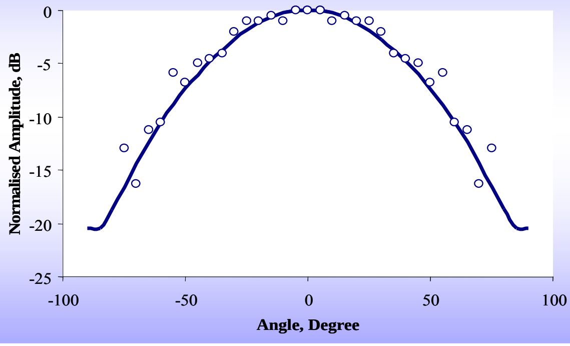

THz MCMs

M. S. Aftanasar, I. Stamatopoulos, **S. Lucyszyn**, S. R. P. Silva and I. D. Robertson, **"Feasibility study of materials for novel millimetre-wave multi-chip modules"**, *Proceedings of the 6th European Conference on MultiChip Modules*, London, UK, Jan. 2000

S. Lucyszyn, S. R. P. Silva, I. D. Robertson, R. J. Collier, A. K. Jastrzebski, I. G. Thayne and S. P. Beaumont, **"Terahertz multi-chip module (T-MCM) technology for the 21st Century?"**, *IEE Colloquium Dig. on Multi-Chip Modules and RFICs*, pp. 6/1-8, May 1998

Commercial MCM Applications for 75 to 300 GHz

- Collision avoidance radar at 77 GHz
- High resolution radiometric imaging at 94 & 140 GHz
- 'Radio-over-fibre' communications at 180 GHz
- Tagging/identification systems
- Pollution monitoring sensors [109 (O_3),150 (NO_x), 278 (ClO),…GHz]
- Medical sensors for sub-cellular probing
- Optical communications 10 to > 40 Gb/s

Radio Frequency Engineering
Lecture #5 MPRWGs

Miniature MPRWG Technologies

* Monolithic micromachining techniques have been investigated for realising air-filled MPRWG structures at 200 GHz and 1.6 THz

* Potential drawbacks with this micromachining technology are the limitations in design flexibility, poor yield and high production cost.

* Experimental multilayer MPRWGs have been demonstrated.

* In principle the multilayer MPRWG technology allows complete integration of waveguides, lumped elements and microstrips with a fixed process sequence.

Imperial College London ステファン・ルシズィン Stepan Lucyszyn
インペリアル・カレッジ・ロンドン准教授 UT-PSC

Radio Frequency Engineering
Lecture #5 MPRWGs

Conventional MCM Interconnect Technologies

* Conventional wire-bonding is limited to *circa* 30 GHz
* Flip-chip techniques are still only limited to *circa* 100 GHz

Why Not Rectangular Waveguides?

* At mm-wave frequencies, the metal-pipe rectangular waveguide (MPRWG) is the perfect transmission line:
  - Limitation of planar lines (CPW & microstrip) is loss above 100 GHz
  - Advantage of high-Q (low ohmic metal & dielectric losses)
  - Excellent isolation
  - Good power handling

Imperial College London ステファン・ルシズィン Stepan Lucyszyn
インペリアル・カレッジ・ロンドン准教授 UT-PSC

Radio Frequency Engineering
Lecture #5 MPRWGs

Illustration of a Future MCM Transmitter Architecture with Integrated PA

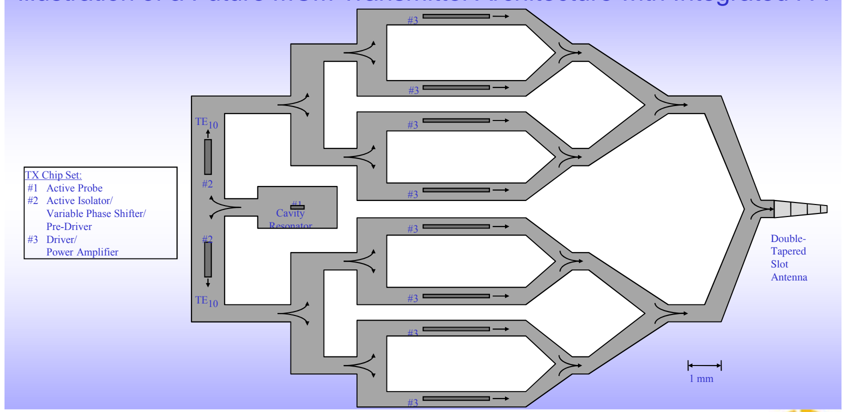

Imperial College London ステファン・ルシズィン Stepan Lucyszyn
インペリアル・カレッジ・ロンドン准教授 UT-PSC

Illustration of Future MCM Receiver Architecture with Antenna Array

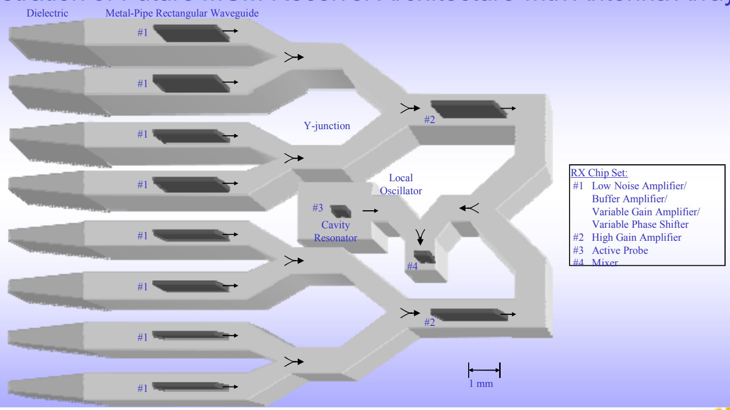

Radio Frequency Engineering
Lecture #5 MPRWGs

24GHz FMCW Radar Front-End System on Substrate
Z. Li and K. Wu, Ecole Polytechnique, Canada, 2007

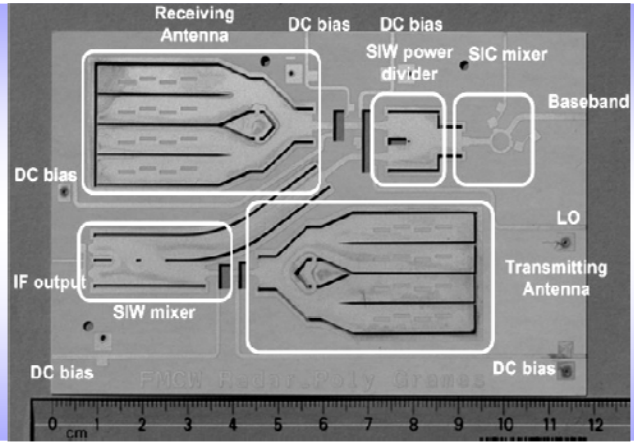

Imperial College London ステファン・ルシズィン Stepan Lucyszyn
インペリアル・カレッジ・ロンドン准教授 UT-PSC

Radio Frequency Engineering
Lecture #5 MPRWGs

Terahertz-Multichip Module Technology (T-MCM)
Simplified Illustrations of a future in-line amplifier assembly

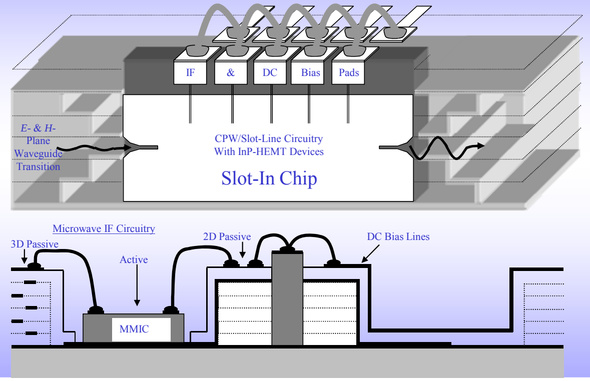

Imperial College London ステファン・ルシズィン Stepan Lucyszyn
インペリアル・カレッジ・ロンドン准教授 UT-PSC

Radio Frequency Engineering
Lecture #5 MPRWGs

RETINA

REconfigurable Terahertz INtegrated Architecture (RETINA)

S. Lucyszyn and Y. Zhou, **"Reconfigurable Terahertz Integrated Architecture (RETINA)",** 33rd International Conference on Infrared, Millimeter, and Terahertz Waves (IRMMW-THz 2008), Pasadena, USA, Sep. 2008

Y. Zhou and **S. Lucyszyn**, "**Modelling of reconfigurable terahertz integrated architecture (RETINA) SIW structures**", EM Academy's PIER Journal, vol. 105, pp. 71-92, Jun. 2010

Imperial College London ステファン・ルシズィン Stepan Lucyszyn
インペリアル・カレッジ・ロンドン准教授 UT-PSC

✍ **At THz frequencies, guided-wave structures and resonators can in general exhibit:**

*** High integration and low cost – at the expense of high losses**

*** Low loss – at the expense of poor integration and high cost**

✍ **At THz frequencies, reconfigurable & multifunctional front-end architectures represents a major challenge:**

*** Prohibitively expensive**

*** Impossible to integrate properly**

✍ Basic material parameters:

- Maximum photoconductivity – represents sidewall losses
- Dark conductivity – represents dielectric losses
- Carrier lifetime – defines the sidewall stability
- Band gap energy – dictates minimum illumination wavelength

✍ **Basic RETINA concept is based on creating virtual side walls**

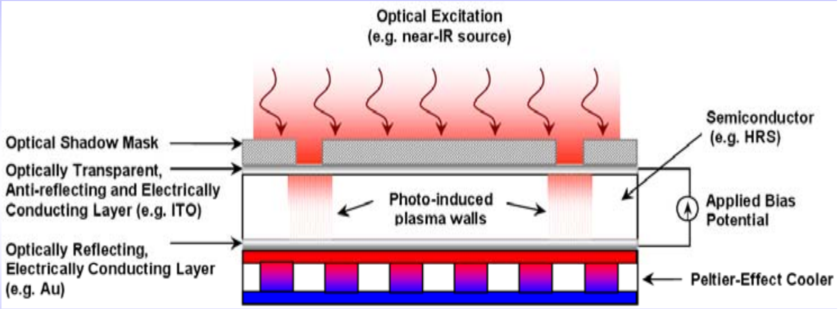

Photoconductivity (PC) effect $\lambda_{opt}(\mu m) \le \dfrac{1.24}{E_g(eV)}$

✍ **Conventional and new materials**:

Material	Carrier Lifetime [s]	Band gap energy [eV]	Dark Conductivity [S/cm]	Maximum Photoconductivity [S/cm]
HRS	**10^{-4}**	**1.1**	**10^{-3}**	**> 1000**
Ge	10^{-4}	0.67	10^{-2}	>600
GaAs	10^{-7}	1.43	10^{-2}	>100
CdSe	10^{-4}	1.7	10^{-7}	2.77
α-Si:H	-	0.7-0.8 (activation energy of conduction)	10^{-9}-10^{-8}	10^{-3}-10^{-2}
(Semi-)Conducting Polymers				

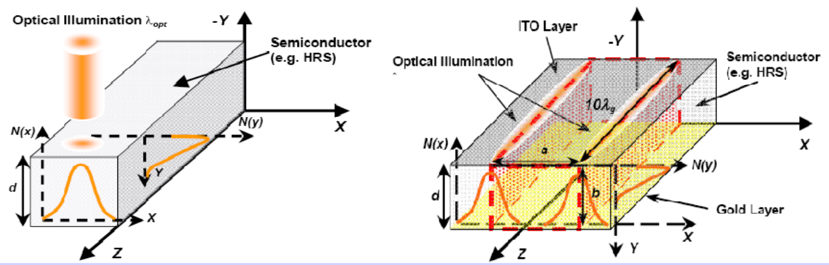

Radio Frequency Engineering
Lecture #5 MPRWGs

Continuous Wave PC Effect

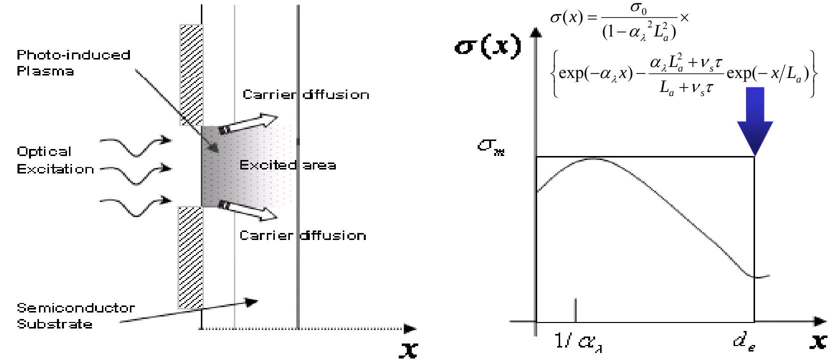

$$\sigma(x) = \frac{\sigma_0}{(1-\alpha_\lambda{}^2 L_a^2)} \times \left\{ \exp(-\alpha_\lambda x) - \frac{\alpha_\lambda L_a^2 + v_s \tau}{L_a + v_s \tau} \exp(-x/L_a) \right\}$$

Imperial College London
ステファン・ルシズィン Stepan Lucyszyn
インペリアル・カレッジ・ロンドン准教授
UT-PSC

Radio Frequency Engineering
Lecture #5 MPRWGs

Picosecond Pulse PC Effect

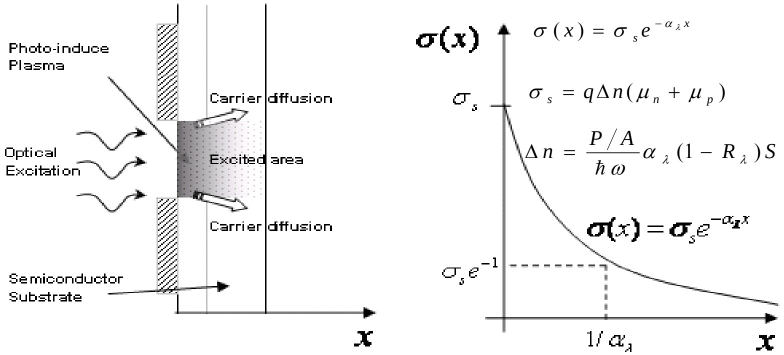

$$\sigma(x) = \sigma_s e^{-\alpha_\lambda x}$$

$$\sigma_s = q \Delta n (\mu_n + \mu_p)$$

$$\Delta n = \frac{P/A}{\hbar \omega} \alpha_\lambda (1 - R_\lambda) S$$

$$\sigma(x) = \sigma_s e^{-\alpha_\lambda x}$$

Imperial College London
ステファン・ルシズィン Stepan Lucyszyn
インペリアル・カレッジ・ロンドン准教授
UT-PSC

Radio Frequency Engineering
Lecture #5 MPRWGs

Silvaco™ TCAD simulations: 2D Luminous

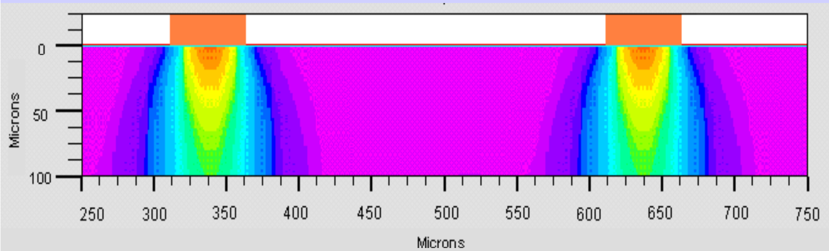

Beam Width = 50 μm
Wafer Thickness = 100 μm
Optical Incident Power Range: 10-100 W/cm^2

Imperial College London
ステファン・ルシズィン Stepan Lucyszyn
インペリアル・カレッジ・ロンドン准教授
UT-PSC

Radio Frequency Engineering
Lecture #5 MPRWGs

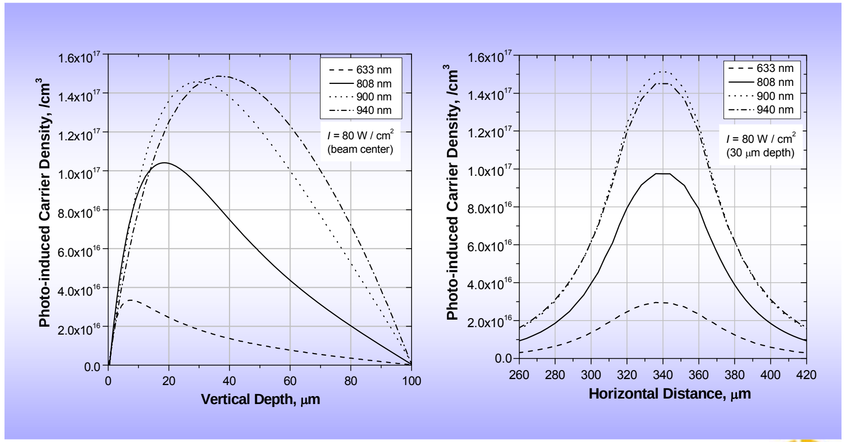

Imperial College London ステファン・ルシズィン Stepan Lucyszyn
インペリアル・カレッジ・ロンドン准教授
UT-PSC

Radio Frequency Engineering
Lecture #5 MPRWGs

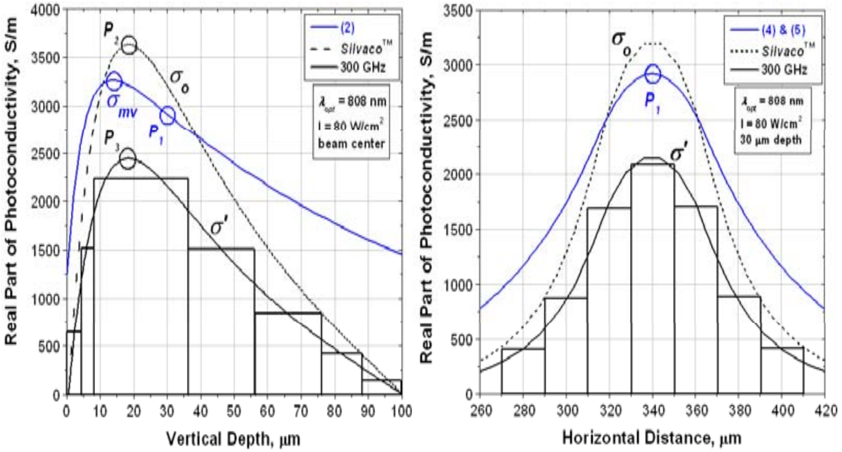

Imperial College London ステファン・ルシズィン Stepan Lucyszyn
インペリアル・カレッジ・ロンドン准教授
UT-PSC

Radio Frequency Engineering
Lecture #5 MPRWGs

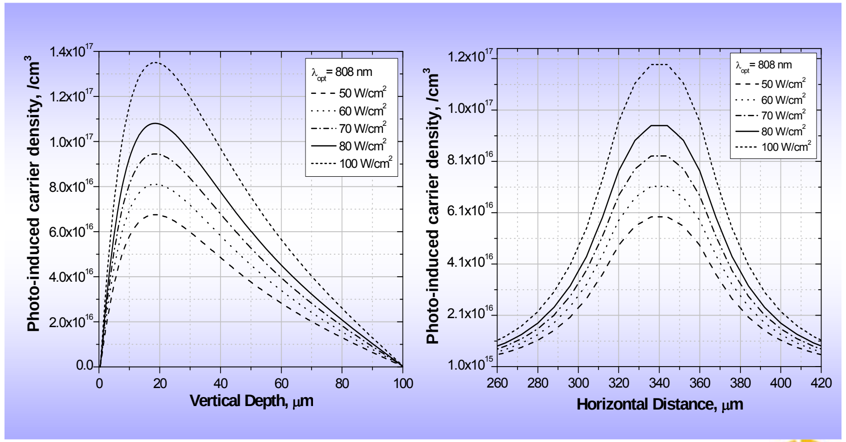

Imperial College London ステファン・ルシズィン Stepan Lucyszyn
インペリアル・カレッジ・ロンドン准教授
UT-PSC

Radio Frequency Engineering
Lecture #5 MPRWGs

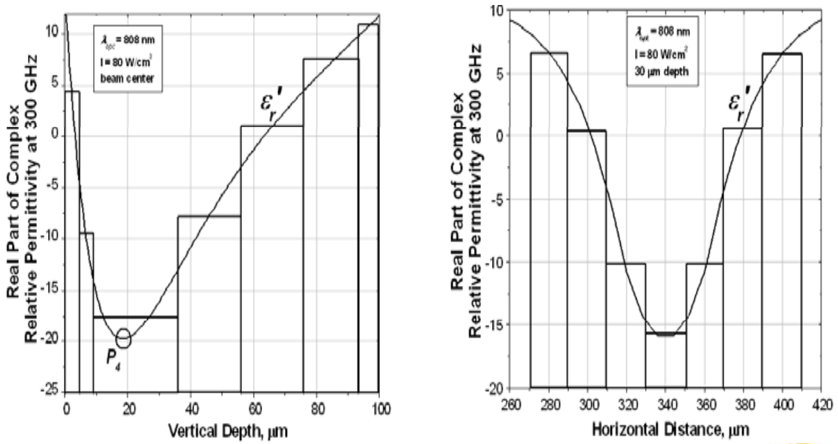

Imperial College London ステファン・ルシズィン Stepan Lucyszyn
インペリアル・カレッジ・ロンドン准教授
UT-PSC

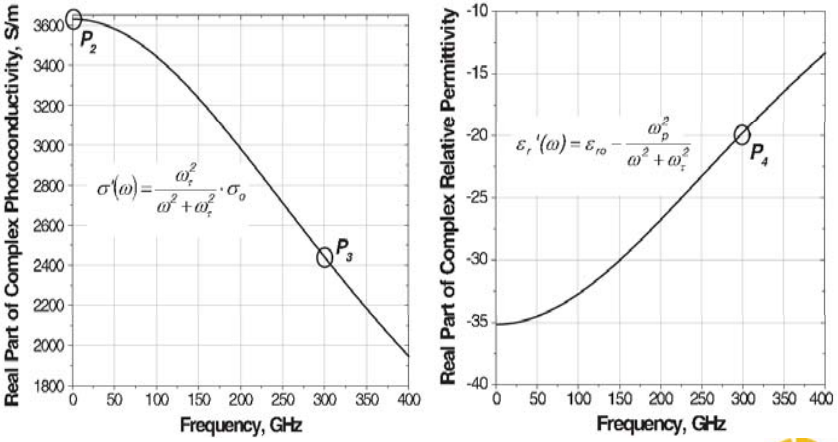

Wall Permittivity Modelling

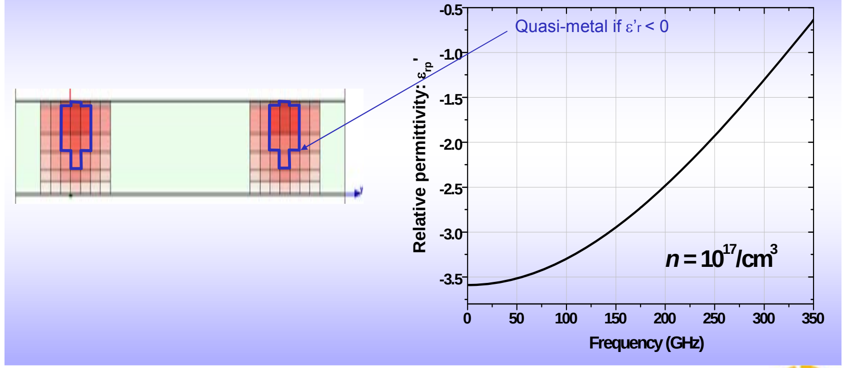

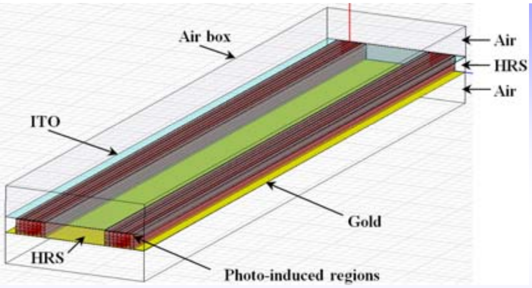

Single Sided

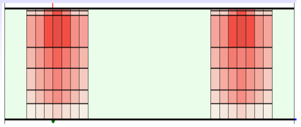

Double Sided

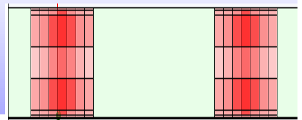

HFSS™ simulations: comparison with two beams

Single Sided at 300 GHz

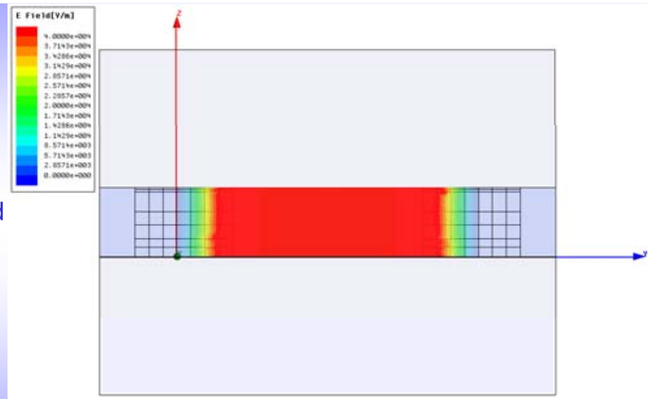

✍ Double Sided at 300 GHz

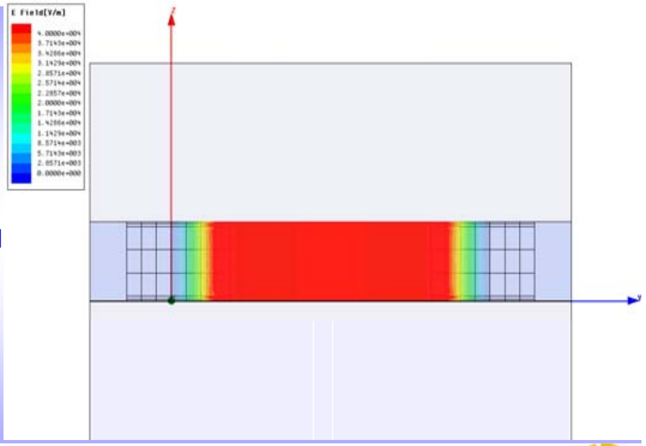

Equivalent Solid Wall

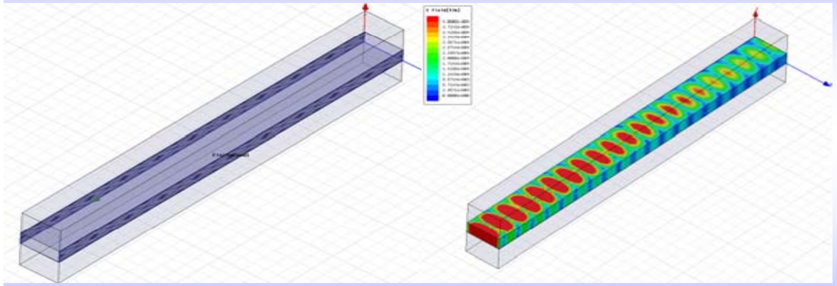

TE10 mode E-field Plots at 300 GHz

✍ Single Sided ✍ Double Sided

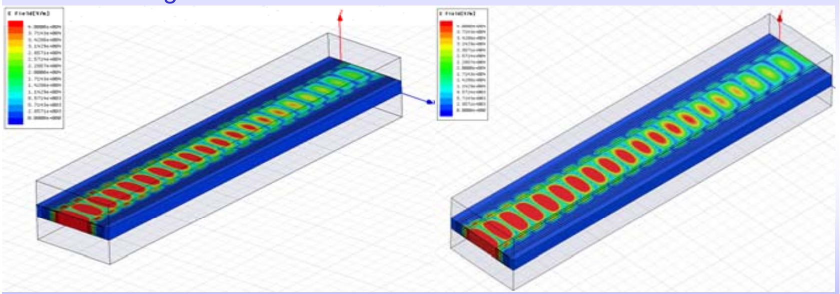

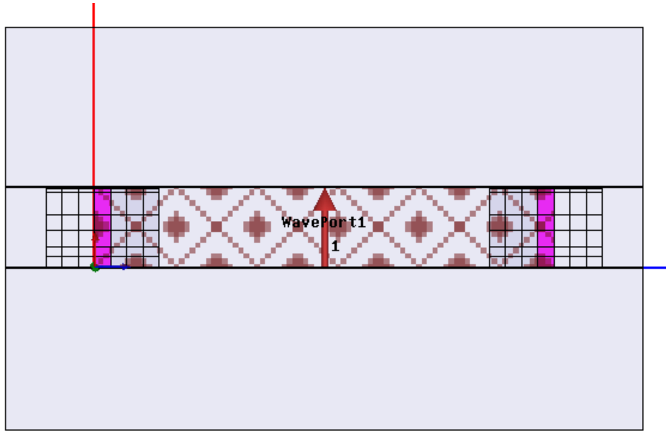

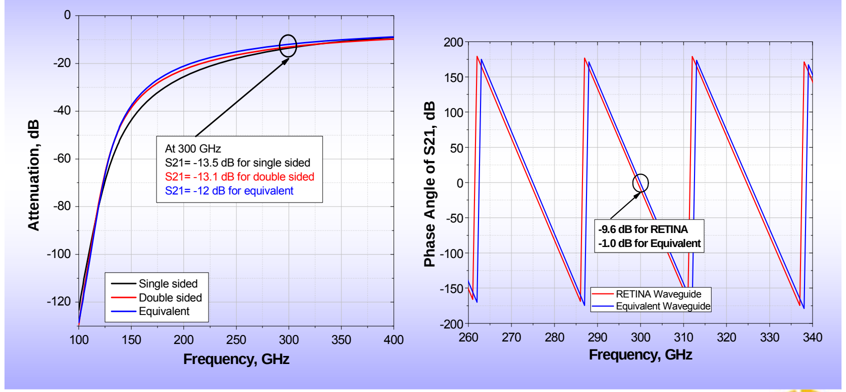

Radio Frequency Engineering
Lecture #5 MPRWGs

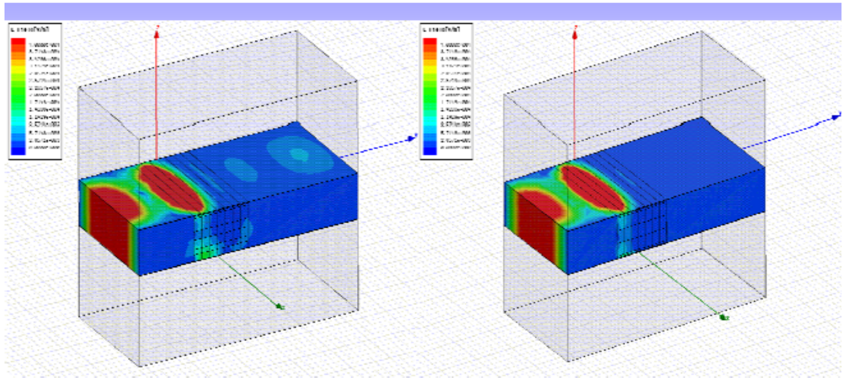

Imperial College London ステファン・ルシズィン Stepan Lucyszyn
インペリアル・カレッジ・ロンドン准教授 UT-PSC

Radio Frequency Engineering
Lecture #5 MPRWGs

RETINA Wall Characterization

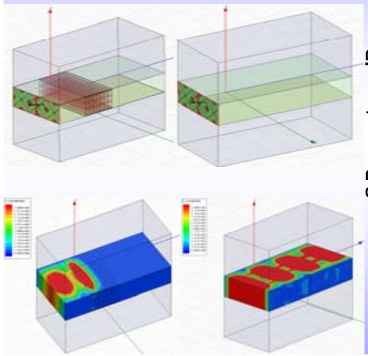

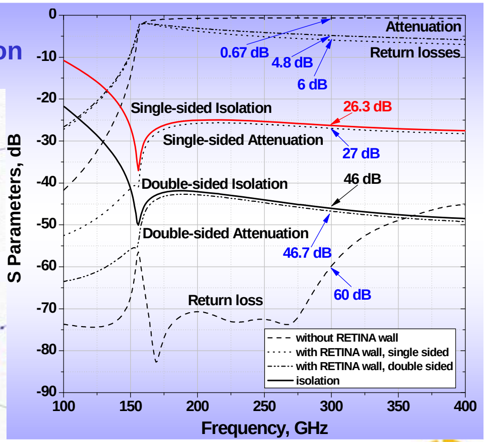

Imperial College London ステファン・ルシズィン Stepan Lucyszyn
インペリアル・カレッジ・ロンドン准教授 UT-PSC

Radio Frequency Engineering
Lecture #5 MPRWGs

Loss Comparison with Various Non-Tuneable/Reconfigurable SIW Technologies

Technology	Frequency (GHz)	Insertion loss (dB/mm)	Conductor loss scaling to 300 GHz (dB/mm)
Alumina SIW	50	0.03	0.07
Ceramic (HT1000) SIW	60	0.20	0.45
Ceramic (QM44F) SIW	74	0.70	1.41
Polyimide (Kapton HN) SIW	79	0.17	0.33
Photoimageable Dielectric HD1000-filled MPRWG	83	1.2	2.3
Air-filled MPRWG	100	0.01	0.017
Polyimide-filled MPRWG	105	8.98	15.18
Air-filled MPRWG	400	0.086	0.074
RETINA (simulated)	300	3.88	3.88

Imperial College London ステファン・ルシズィン Stepan Lucyszyn
インペリアル・カレッジ・ロンドン准教授 UT-PSC

Double Sided RETINA Cavity Resonators

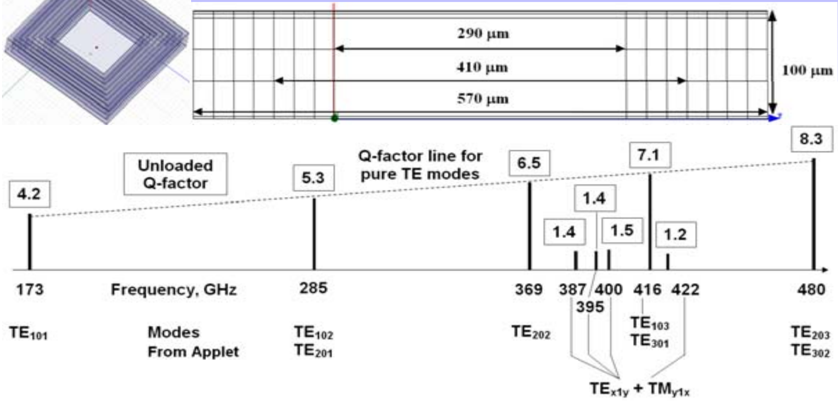

TE_{301} TE_{302}

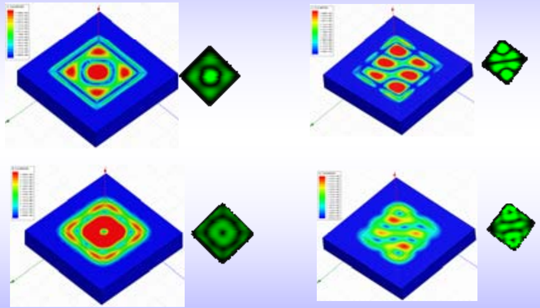

TE_{101} TE_{201} TE_{202}

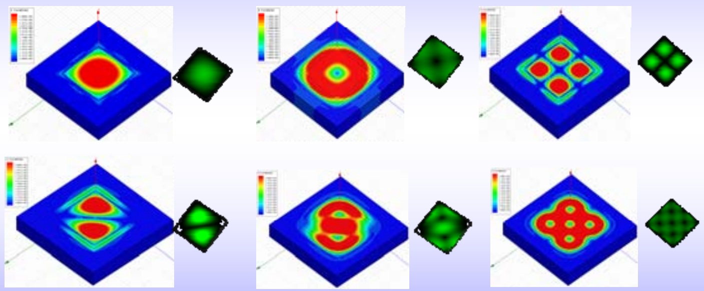

Single Sided Backside for TE_{101} at 170 GHz

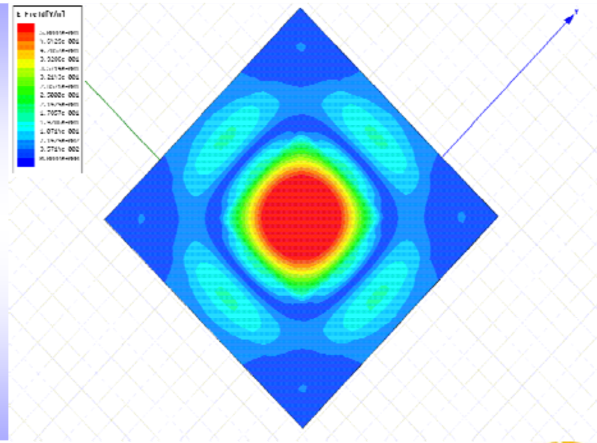

Double Sided Backside for TE_{101} at 173 GHz

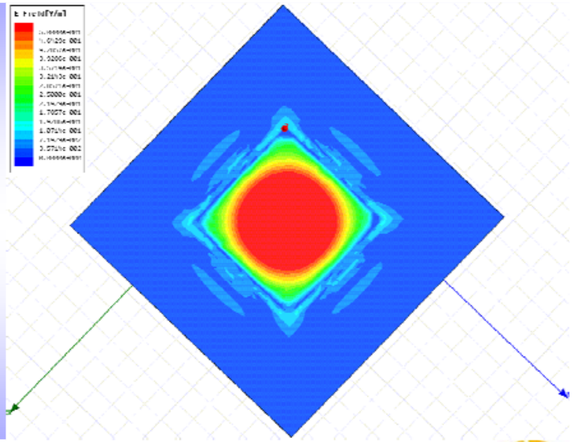

Radio Frequency Engineering
Lecture #5 MPRWGs

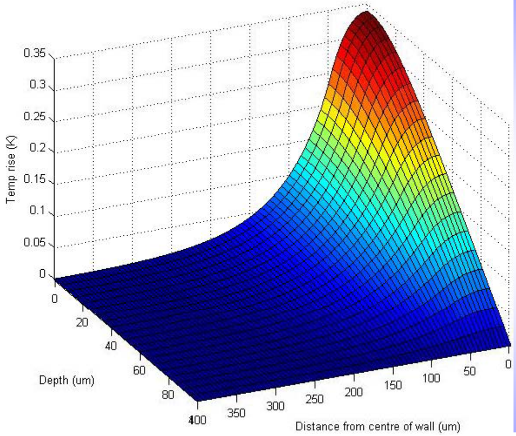

✍Distribution of temperature rise for a 100 μm wide virtual wall in a 100 μm thick substrate, assuming:

- 80 W/cm² incident power
- good backside heatsink

Temperature rise in the RETINA substrate could be kept below 1 °C under realistic illumination conditions

Imperial College London ステファン・ルシズィン **Stepan Lucyszyn** インペリアル・カレッジ・ロンドン准教授 UT-PSC

Radio Frequency Engineering
Lecture #5 MPRWGs

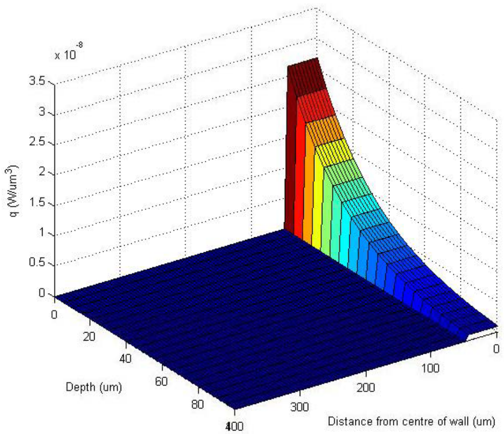

✍ Using 2D finite difference solver in Matlab:

Distribution of heat generation due to light absorption, assuming:

- absorption length of 30 μm
- no reflection at the bottom of the substrate

Imperial College London ステファン・ルシズィン **Stepan Lucyszyn** インペリアル・カレッジ・ロンドン准教授 UT-PSC

Radio Frequency Engineering
Lecture #5 MPRWGs

✍ Simple proof-of-concept experiment at 200 GHz

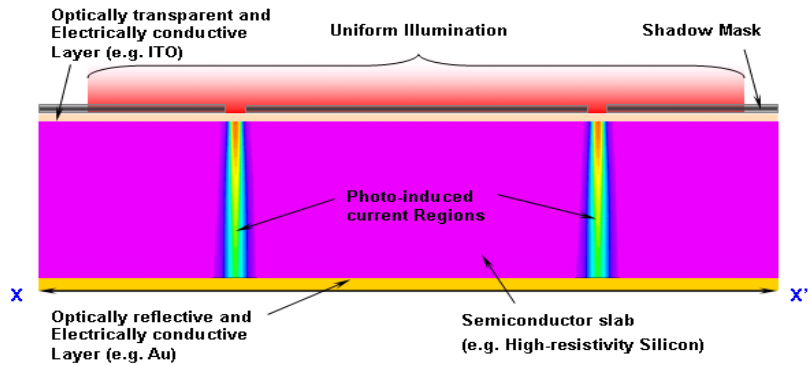

Imperial College London ステファン・ルシズィン **Stepan Lucyszyn** インペリアル・カレッジ・ロンドン准教授 UT-PSC

✍ MPRWG design for conventional on-wafer probing at 200 GHz

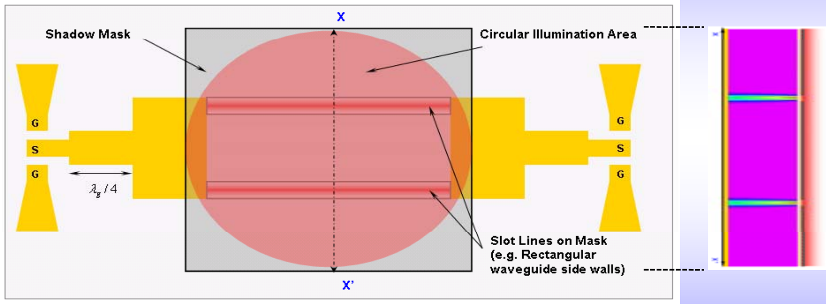

✍ Tuneable RETINA filters, with λg/2 resonant cavities coupled by inductive irises

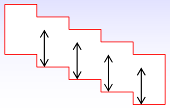

Other tuneable RETINA exemplars:
* Variable power splitters
* Tuneable short circuit stubs
* Variable delay line
* Radiating tapered horn antennas

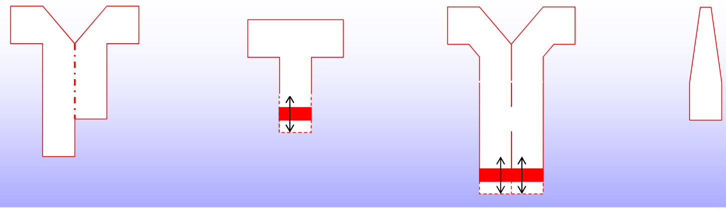

✍ RETINA exemplars:
- right-angled bends
- power splitters
- SP3T switches

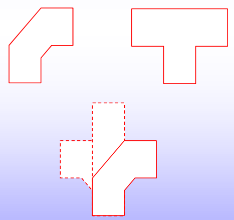

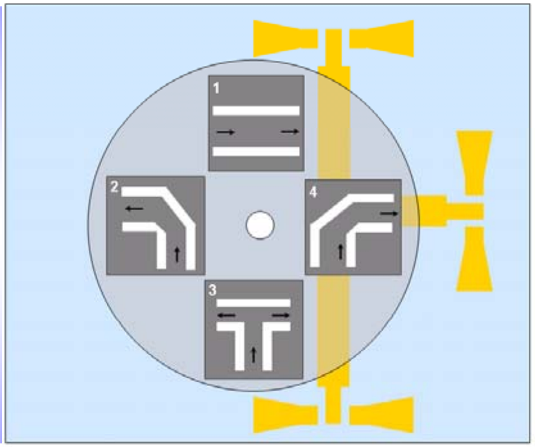

✍ Scanning phased array antenna demonstrator at 200 GHz

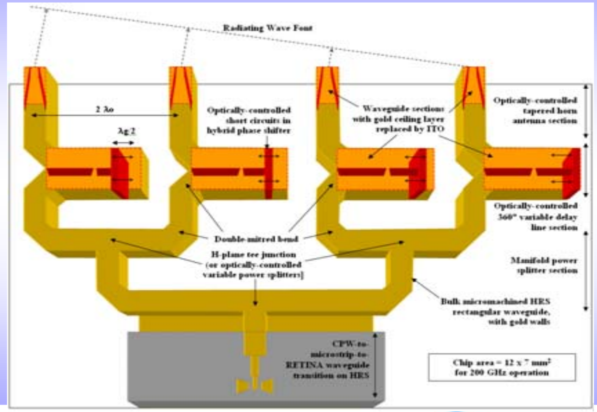

✍ **The pattern of incident light can be controlled in a number of ways**

Proximity shadow mask
- Very inefficient, with almost all incident optical power being wasted
- Non-tuneable components only
- Reasonable approach for an initial demonstration

"Clever" Bespoke refractive or diffractive optics
- very efficient
- non-tuneable components only

Phase-modulated SLM
- 90% light utilization efficiency.
- Commercial liquid crystal on silicon (LCOS) SLMs, appear to be ideally suited for this application

Scanned focused laser
- Spot writing time for the complete pattern would have to be smaller than the electron-hole pair recombination time
- Challenging for large/complex architectures

Spatial Light Modulator (SLM)
e.g. replacing the white light source in a Texas Instruments DLP® projector by a near-IR laser source:

- Versatile illuminator that could be interfaced with a PC
- Programmed using even a simple drawing package
- Power handle issues, with dumped energy
  i.e. the energy not transmitted to the substrate

RETINA can provide:	**Loss Reduction Techniques:**
Integration	Bespoke transparent conductive oxide
Reconfigurability	Optimize substrate/wavelength/power
Tunability	Double-sided exposure
At the Expense of:	Over-sized waveguide
Increased Losses	Superposition of CW and pulse excitation?
Increased Complexity (Clever Optics)	

Paradigm shift in THz integration

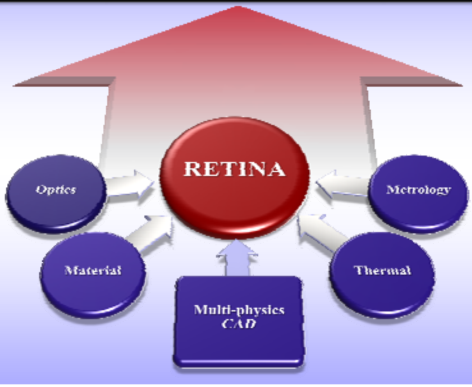

Radio Frequency Engineering
Lecture #5 MPRWGs

Conclusions

System-on-Chip continues to advance rapidly but technological restrictions inherent

System-in-Package is the ideal compromise

Amazing advances in 3D packaging and improved materials gives great opportunities for millimetre-wave applications

Perhaps, light needs to be shone on the subject?

Imperial College London
ステファン・ルシズィン **Stepan Lucyszyn**
インペリアル・カレッジ・ロンドン准教授
UT-PSC